

1

Upscaling aquifer storage 2 and recovery (ASR)

3 A northern Ghana multiple case study
4 on small scale agriculture

5 by

6 Frank J. van den Toorn

7 to obtain the degree of Master of Science
8 at the Delft University of Technology,
9 to be defended publicly on Tuesday January 1, 2013 at 10:00 AM.

10 Student number: 4179404
Project duration: September 18, 2017 – July 1, 2018
Thesis committee: Prof. dr. ir. M. Bakker, TU Delft (Chair)
Prof. dr. ir. N.C. van de Giesen, TU Delft
Dr. ir. J.S. Timmermans, TU Delft
Ir. D.A. Brakenhoff, Witteveen+Bos

11 An electronic version of this thesis is available at <http://repository.tudelft.nl/>.



Preface

14 This thesis accommodates the final product in becoming a Master of Science in Watermanagement at the
 15 Delft University of Technology - faculty of Civil Engineering and Geosciences. I would like to acknowledge
 16 all the people who contributed to my graduation. Some however do deserve a special emphasis. First of
 17 all, I would like to thank the entire committee for assessing my thesis. Subsequently I would like to give
 18 a word of gratitude to Witteveen+Bos - Herman Mondeel & Davíd Brakenhoff - for the abundant research
 19 facilities and daily supervision. And last but not least I owe Conservation Alliance - Paa Kofi Osei-Owusu -
 20 a special gratitude. Without the cooperation of CA the fieldwork data collection within the northern Ghana
 21 local communities would not have been possible.

22
23

*Frank J. van den Toorn
Delft, July 2018*



Summary

25 bllaa bbllaa

26

27 enzovort

Contents

29	List of Figures	ix
30	List of Tables	xi
31	1 Introduction	1
32	1.1 Northern Ghana characteristics	1
33	1.2 ASR systems	1
34	1.3 PIT & Irrigation purpose	1
35	2 Fieldwork data analysis	5
36	2.1 Parameter derivation methods	6
37	2.1.1 Theoretical model definition	6
38	2.1.2 Techniques in analysis	6
39	2.1.3 Optimization functions	7
40	2.2 From fieldwork data to T & S values	8
41	2.2.1 Location: Bingo	8
42	2.2.2 Location: Nungo	9
43	2.2.3 Location: Nyong Nayili	9
44	2.2.4 Location: Janga (1/2)	10
45	2.2.5 Location: Janga (2/2)	10
46	2.2.6 Location: Ziong (monitoring)	11
47	2.3 Theoretical validation	11
48	2.4 Fieldwork results	11
49	3 Model scenarios	13
50	3.1 Scenarios	13
51	3.2 Test criteria	13
52	3.3 Run	13
53	3.4 Results & Conclusions	13
54	4 (Financial) yields - upscaling	15
55	4.1 inhoud	15
56	5 Conclusions	17
57	6 Discussion & Recommendations	19
58	Bibliography	21
59	Appendices	23
60	A Original Borehole Logsheets	25
61	B Fieldwork set-up	31
62	B.1 Equipment	31
63	B.2 General measurement structure	33
64	B.3 Site-specific measurement results	36
65	C Extense report - Fieldwork data analysis	43
66	C.1 Bingo - overview	44
67	C.2 Nungo - overview	46
68	C.3 Nyong Nayili - overview	47
69	C.4 Janga first attempt - overview	49

70	C.5 Janga second attempt - overview	51
71	C.6 Ziong - overview	53
72	D Modflow radial conversion	55
73	D.1 Test 1: Steady flow to a fully penetrating well in confined aquifer	58
74	D.2 Test 2: Steady flow to a fully penetrating well in unconfined aquifer	60
75	D.3 Test 3: Unsteady flow to a partially penetrating well in unconfined aquifer	62

List of Figures

77	1.1 Example on (a) flood near Weisi, Upper West Region and (b) drought near Nungo, Upper East Region	2
78	1.2 Principle Aquifer Storage & Recovery (ASR) system	3
79	1.3 Schematic: dry season system use	3
80	1.4 Schematic: desired up-scaling in dry season system use	3
82	2.1 Overview of fieldwork locations in northern Ghana	5
83	2.2 Schematic cross-sectional view of (a) generalized northern Ghana soil stratification and sim- plified representations: (b) a single layer system, (c) a double layer system, and (d) a system with two layers and partial penetration of the well	6
85	2.3 Bingo - multi-layer best fits	9
87	2.4 Nyong Nayili - multi-layer best fits	10
88	2.5 Janga first attempt - multi-layer best fits	10
89	2.6 Janga second attempt - multi-layer best fits	10
90	2.7 Ziong - multi-layer best fits	11
91	B.1 Comparable example of the fieldwork submersible pump	31
92	B.2 Comparable example of the fieldwork generator	32
93	B.3 Actual fieldwork hose & bucket	32
94	B.4 Comparable examples of Van Essen TD- & Baro-Divers	33
95	B.5 Comparable examples of In-Situ TD- & Baro-Divers	33
96	B.6 Comparable example of the fieldwork water tape	34
97	B.7 Fieldwork (measurement) set-up (a) general, (b) simplified	35
98	B.8 Fieldwork fact-sheet: Bingo	37
99	B.9 Fieldwork fact-sheet: Nungo	38
100	B.10 Fieldwork fact-sheet: Nyong Nayili	39
101	B.11 Fieldwork fact-sheet: Janga (attempt 1)	40
102	B.12 Fieldwork fact-sheet: Jamga (attempt 2)	41
103	B.13 Fieldwork fact-sheet: Ziong (location of monitoring)	42
104	C.1 Bingo single layer fieldwork data analysis by the optimization (a) fmin-RMSE method and (b) TTim calibration method	44
105	C.2 Bingo double layer fieldwork data analysis by the optimization (a) fmin-RMSE method and (b) TTim calibration method	44
106	C.3 Bingo partially penetrating double layer fieldwork data analysis by the optimization (a) fmin- RMSE method and (b) TTim calibration method	45
107	C.4 Nyong Nayili single layer fieldwork data analysis by the optimization (a) fmin-RMSE method and (b) TTim calibration method	47
108	C.5 Nyong Nayili double layer fieldwork data analysis by the optimization (a) fmin-RMSE method and (b) TTim calibration method	47
109	C.6 Nyong Nayili partially penetrating double layer fieldwork data analysis by the optimization (a) fmin-RMSE method and (b) TTim calibration method	48
110	C.7 Janga first attempt single layer fieldwork data analysis by the optimization (a) fmin-RMSE method and (b) TTim calibration method	49
111	C.8 Janga first attempt double layer fieldwork data analysis by the optimization (a) fmin-RMSE method and (b) TTim calibration method	49

120 C.9 Janga first attempt partially penetrating double layer fieldwork data analysis by the optimiza-	50
121 tion (a) fmin-RMSE method and (b) TTim calibration method	
122 C.10 Janga second attempt single layer fieldwork data analysis by the optimization (a) fmin-RMSE	51
123 method and (b) TTim calibration method	
124 C.11 Janga second attempt double layer fieldwork data analysis by the optimization (a) fmin-RMSE	51
125 method and (b) TTim calibration method	
126 C.12 Janga second attempt partially penetrating double layer fieldwork data analysis by the opti-	52
127 mization (a) fmin-RMSE method and (b) TTim calibration method	
128 C.13 Ziong single layer fieldwork data analysis by the optimization (a) fmin-RMSE method and (b)	53
129 TTim calibration method	
130 C.14 Ziong double layer fieldwork data analysis by the optimization (a) fmin-RMSE method and (b)	53
131 TTim calibration method	
132 C.15 Ziong partially penetrating double layer fieldwork data analysis by the optimization (a) fmin-	54
133 RMSE method and (b) TTim calibration method	
134 D.1 Schematic of an axially symmetric model (Langevin, 2008)	55
135 D.2 Modflow topview schematisation of a: (a) Rectangular model, (b) Rectangular round model	
136 and (c) Single row model	57
137 D.3 Schematic test 1	58
138 D.4 Results test 1	59
139 D.5 Schematic test 2	60
140 D.6 Results test 2	61
141 D.7 Schematic test 3	62
142 D.8 Results test 3: Cross-section head contour after 1 day of pumping	62
143 D.9 Results test 3: Head after 1 day of pumping at 2.0m (relative to aquifer bottom)	63

List of Tables

144

145	2.1 Bingo - overview best fit parameters	9
146	2.2 Nyong Nayili - overview best fit parameters	9
147	2.3 Janga first attempt - overview best fit parameters	10
148	2.4 Janga second attempt - overview best fit parameters	11
149	2.5 Ziong - overview best fit parameters	11

150

151

Introduction

152 **1.1. Northern Ghana characteristics**

153 Ghana's northern part climate is labelled as semi-arid savannah-like. High temperatures are common and
154 on a yearly basis the short rainy season is out-performed by long periods of drought. As a source of water
155 supply, groundwater is abstracted from its surroundings. The relatively high-quality water is collected and
156 mainly used for domestic purposes, livestock and construction. In more restricted quantities groundwater
157 is used for irrigation. The use of groundwater prevents farmers from incurring potential losses in crop pro-
158 duction and increases yields.

159 For as long as natural recharge rates exceed discharge, the used groundwater is renewable and the water
160 source is stated to be sustainable. It is roughly estimated the environment has the capability to naturally
161 recharge a maximum of 2.5-10% of the annual rainfall. Based on the rainfall data for northern Ghana this
162 results in an estimated long term annual natural recharge of 60 mm/y. Currently, local groundwater use is
163 estimated to be approximately 5% of this annual recharge (Martin, 2006). The amount of water withdrawn is
164 marginal and the environment is therefore self-reliant. However, fluctuations in groundwater use over time
165 and place do occur. Accurate field data on these fluctuations is lacking. Recent observations show wells
166 drying out and groundwater tables falling, both indicators of possible unsustainable groundwater use.

167 Following the trend seen in previous decades, it is expected future groundwater production will further
168 increase. An overall improvement of the Ghanaian energy network as well as lower energy costs will make
169 groundwater more accessible via electrical pumps. In general, this will lead to more extensive use of ground-
170 water in the ongoing battle against shortages in clean drinking water. On top of this the national government
171 aims at becoming more self-sufficient. Policies are pointed at more intensive agricultural development in
172 the northern regions of Ghana (Wood, 2013). Optimization in field irrigation has the potential to increase
173 yields and even double the number of crops produced per year (Owusu et al., 2017). Consequently, the need
174 for groundwater abstraction becomes substantially higher. Climate change can potentially have a negative
175 influence on the natural recharge. While the need will be higher, natural recharge volumes can become
176 lower. In the near future it is possible that discharge rates will exceed natural recharge and the abstracting
177 of groundwater is no longer sustainable. Objective of this research is to explore the possibilities of scaling
178 up artificially managed aquifer recharge (MAR) for aquifer storage and recovery (ASR) to contribute towards
179 the continued sustainable use of groundwater in the northern regions of Ghana.

180 **1.2. ASR systems**

181 blabla

182

183 **1.3. PIT & Irrigation purpose**

184 PIT application on irrigation (single figure). and the desired upscaling of this system (multiple figure).
185 resulting in a research question



(a)



(b)

Figure 1.1: Example on (a) flood near Weisi, Upper West Region (source: Owusu et al., 2017) and (b) drought near Nungo, Upper East Region

186 **Background**

187 **Research gap**

188 **Research purpose**

189 **Research question**

190 How can scaled-up Aquifer Storage and Recovery (ASR) systems be beneficial for the availability and sus-
191 tainable use of agricultural groundwater in northern Ghana?

192

193 How can scaled-up Aquifer Storage and Recovery (ASR) systems be beneficial for the availability and sus-
194 tainable use of groundwater in northern Ghana agriculture?

195 **Reader's guide** to answer this research question...

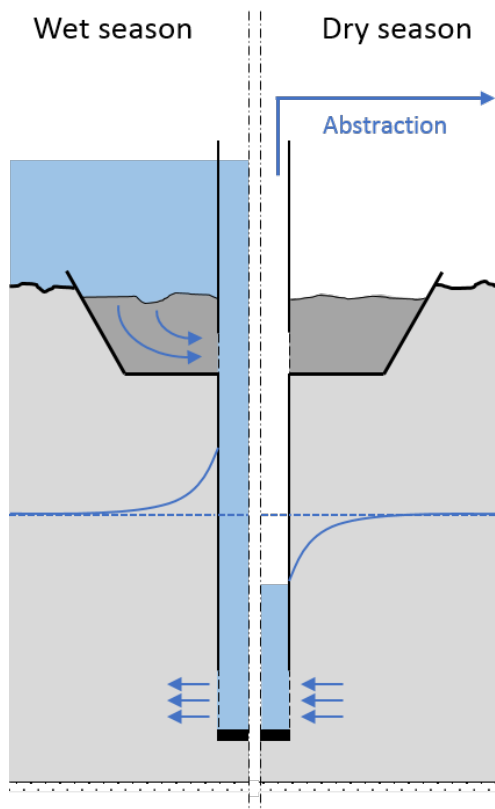


Figure 1.2: Principle Aquifer Storage & Recovery (ASR) system

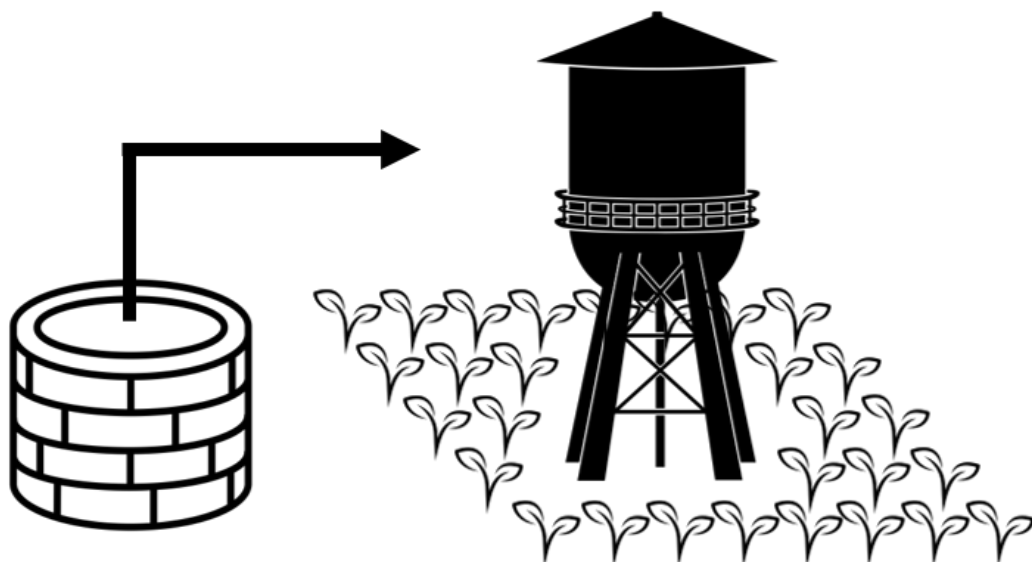


Figure 1.3: Schematic: dry season system use
(visual support by Housin Aziz, Jhun Capaya and Nibras@design from Noun Project - <https://thenounproject.com>)



Figure 1.4: Schematic: desired up-scaling in dry season system use
(visual support by Housin Aziz, Jhun Capaya and Nibras@design from Noun Project - <https://thenounproject.com>)

2

196

197

Fieldwork data analysis

198 Geological conditions are highly heterogeneous in northern Ghana. Subsurface characteristics vary at short
199 mutual distances. Adequate and reliable information about local geohydrological conditions is preferably
200 gathered through site-specific fieldwork. In this research perspective, multiple northern Ghana borehole
201 locations are subjected to groundwater pumping tests.

202 The NGO Conservation Alliance (CA) installed several PIT locations in the summer of 2016, in the Upper
203 East and Northern Region. Pumping tests are performed at four of these boreholes. A fifth PIT borehole (in
204 Ziong) is monitored to study how the ASR system is used by local farmers. The figure below shows a map of
205 the research locations in northern Ghana (Figure 2.1).

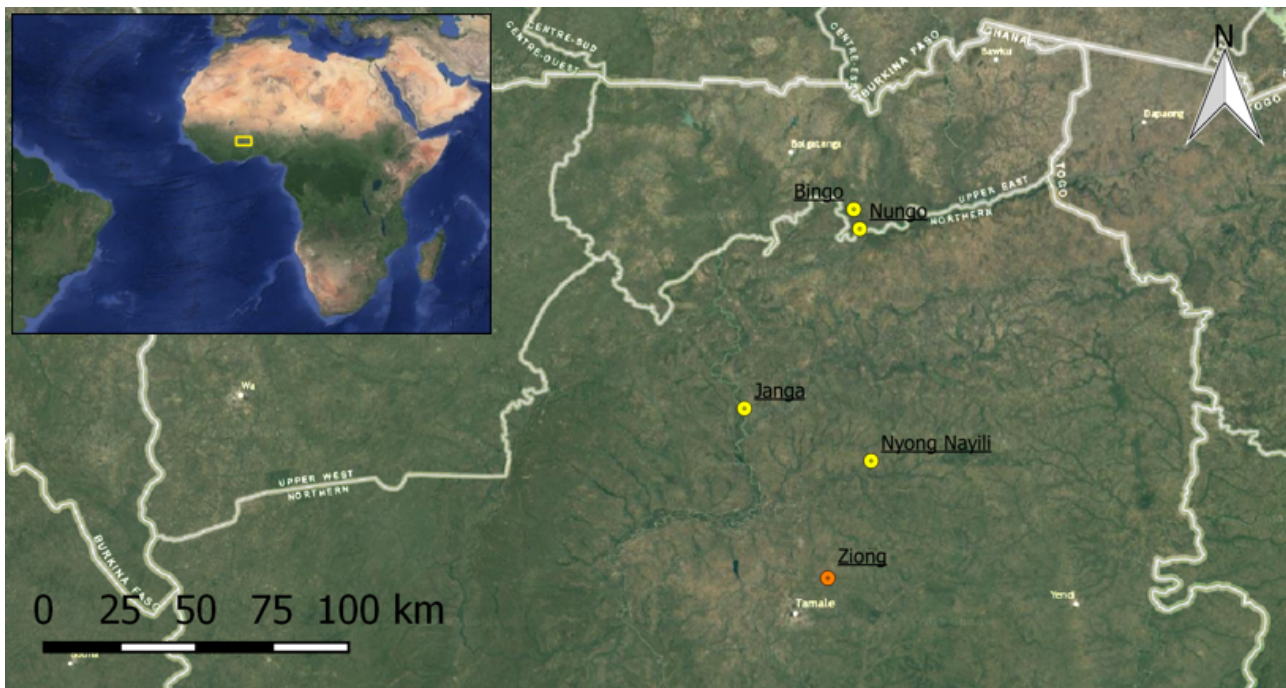


Figure 2.1: Overview of fieldwork locations in northern Ghana

206 Detailed information on the equipment that was used, the set-up of the pumping tests as well as the mon-
207 itoring of an operating ASR system can be found in appendix B. The obtained raw fieldwork data can be
208 found in the site-specific fact-sheets of appendix B.3. The purpose of this fieldwork is to determine geo-
209 hydrological subsurface parameters, transmissivity (T) and storativity (S), which are used as input for further
210 investigation into upscaling these systems.

211 This chapter contains the analysis of gathered fieldwork data. First, the methodology for data analysis,
212 including some theoretical background, is explained (section 2.1). Section 2.2 contains the derivation of

213 the local geohydrological parameter values: T and S . Finally, the chapter concludes with the determination
 214 of parameter bandwidths (section 2.4) which will be used in further model simulations to investigate the
 215 upscaling of ASR systems in northern Ghana.

216 2.1. Parameter derivation methods

217 2.1.1. Theoretical model definition

218 In large parts of the northern Ghana the geohydrological soil characteristics are unknown. Strong variations
 219 in the local geological conditions make it necessary to obtain information about local soil stratification. The
 220 most reliable site-specific information was recorded during the drilling of boreholes (2016). The borehole
 221 log-sheets (appendix A) are used as a starting point for the construction of the theoretical models.

222 Despite differences in soil types, the research locations show similarities in stratification. In each case the
 223 upper 50 meters is divided into two or three layers, consisting of a confining top layer, and below that one
 224 or two "aquifers". Groundwater tables are predominantly positioned in the first aquifer. Based on these
 225 observations three simplified theoretical models for the analysis of fieldwork data are derived, as depicted
 226 in figure 2.2.

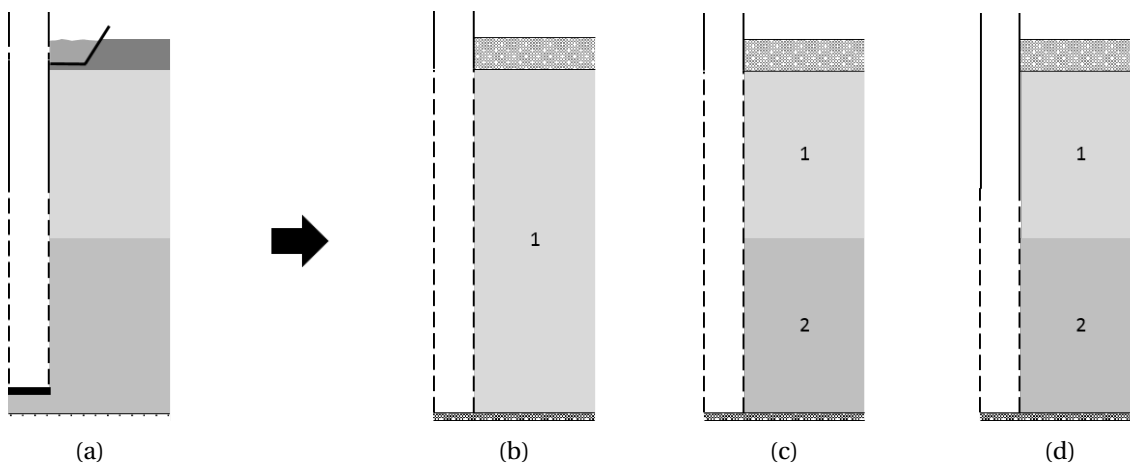


Figure 2.2: Schematic cross-sectional view of (a) generalized northern Ghana soil stratification and simplified representations: (b) a single layer system, (c) a double layer system, and (d) a system with two layers and partial penetration of the well

228 These simplified models (2.2b - 2.2d) mimic local conditions, making the derivation of representative hy-
 229 drdraulic subsurface characteristics (T and S) possible (Kruseman & de Ridder, 2000). Adding more layers
 230 provides more degrees of freedom which potentially leads to a more accurate simulations with double lay-
 231 ered models. However, a maximum of two soil layers are implemented to limit chances of equifinality.
 232

233 2.1.2. Techniques in analysis

234 An increase in the number of layers requires more complex methods for the derivation of parameters.
 235 This section contains a detailed description of techniques applied for the derivation of (multiple) hydraulic
 236 groundwater parameters.

237 Theis's method

238 Groundwater drawdown due to the withdrawal of water can be determined analytically with Theis's equa-
 239 tion (Equation 2.1). Theis's method is applicable on the situation depicted in 2.2b; a constant rate pumping
 240 test in a fully penetrating well in a confined single layer aquifer (Kruseman & de Ridder, 2000). The analytical
 241 solution is suitable for obtaining a first indication of geohydrological parameters.

$$s = \frac{Q}{4\pi K D} \exp(-u) \quad (2.1)$$

$$u = \frac{r^2 S}{4 K D t} \quad (2.2)$$

243 Where s (m) is the drawdown at distance r (m) from the well, Q (m^3) is the constant well discharge , KD
 244 (m^2/d) is the aquifer transmissivity ($KD = T$), S (-) is the aquifer storativity, t (d) is the time measured from
 245 the start of pumping and $\exp1$ is the exponential integral. The drawdown measurements in this research
 246 are limited to in-well measurements. The distance r in Theis's equation is assumed to be the length of the
 247 well radius (0.0635 m). Theis's method is applicable for the time of pumping as well as the recovery process.
 248 The script below shows the implementation of Theis's method in Python.

```
249
250
251 def drawdown(t, T, S):
252     s = Qo / (4 * np.pi * T) * exp1(ro ** 2 * S / (4 * T * t))
253     s[t > toff] -= Qo / (4 * np.pi * T) * exp1(ro ** 2 * S / (4 * T * (t[t>toff] -
254                                         toff)))
255
256     return s
```

257 Analytic Element Modelling in TTIm

258 TTIm is a computer program based on analytic elements and designed for the analysis of transient ground-
 259 water flow in one or more layers. Multiple elements (and types of elements) can be added to specific pre-
 260 defined model layers. The use of TTIm makes it possible to take additional well characteristics into account.
 261 Groundwater heads can be determined inside the well and the model optionally accounts for borehole stor-
 262 age and well skin resistance. Well discharge can be toggled on and off multiple times. This allows simula-
 263 tions of both single pumping and recovery tests and long term well operation.

264 The analysis of the pumping and recovery tests is performed with the TTIm Model3D configuration. The
 265 inclusion of a single well element is sufficient in this case. Depending on which subsurface model is used
 266 (2.2) the well (analytic element) is screened in one or more model layers. The top layer is configured as
 267 phreatic layer, meaning the top layer storage coefficient (S) is a phreatic storage coefficient (S_y). This is
 268 based on observed initial groundwater tables, which Multiplying this value with the aquifer thickness
 269 is therefore no longer needed. Each layer in the model has a thickness of 1 meter. This means derived hy-
 270 drdraulic conductivities (k) can be interpreted as transmissivities (T) and the storage is expressed as the layer
 271 storage coefficient (S). This is done to directly derive T and S values. Additionally, this approach automati-
 272 cally corrects for the unknown thickness of the deepest soil layer in which the well is screened. There is no
 273 information about soil conditions beyond the bottom of the wells in the borehole log-sheets (A).

274 MODFLOW

275 The modelling of upscaling scenario's (see chapter 3) is done with MODFLOW, a finite difference model
 276 for groundwater flow developed by the USGS. MODFLOW is the international standard in groundwater
 277 simulation (bron??). MODFLOW is not used for the derivation of geohydrological parameters. Optimal
 278 parameters derived with TTIm models are implemented in corresponding MODFLOW models to validate
 279 the results obtained with TTIm.

280 2.1.3. Optimization functions

281 Pumping test data (section 2.4) is used as input for the derivation of local geohydrological parameter val-
 282 ues. The values of T and S are determined by fitting the analytical solutions and TTIm models to the data.
 283 In curve fitting process two optimization functions are used.

284 Fmin-RMSE optimization

285 Differences between the measured and modelled drawdown curves can be expressed by the RMSE-value,
 286 equation 2.3 (bron??). The Fmin function is applied (part of Python's scipy.optimize package) to minimize
 287 the difference between modelled and observed drawdowns. This optimization results in optimal T and S
 288 values (and optionally values for borehole storage and well skin resistance) that represent local conditions.
 289 A Python implementation of Fmin optimization is given below. The example shows an optimization of five
 290 parameters (T and S values for two model layers and well skin resistance).

$$RMSE = \sqrt{\sum \frac{(s_{mod} - s_{field})^2}{N}} \quad (2.3)$$

295 Where s_{mod} is the modelled drawdown (m), s_{field} is the observed drawdown (m) and N is the number of data
296 points.

```
297
298
299 def optimTTim_Qvar(params, t, meas):
300     kaq = np.zeros(2)
301     Saq = np.zeros(2)
302     kaq[0] = params[0]
303     kaq[1] = params[1]
304     Saq[0] = params[2]
305     Saq[1] = params[3]
306     res = params[4]
307     s = drawdownTTim_Qvar(t, kaq, Saq, res)
308     error = np.sqrt(np.mean((s-meas)**2))
309     return error
310
311 xopt = fmin(optimTTim_Qvar, x0=[10, 10, .01, .001, 0.1], args=(to[mask], do[mask]),
312             xtol=1e-4)
```

314 Calibration function

315 TTIm also has an in-built calibration function. This optimization function is also applied to improve ro-
316 bustness of the parameter value derivation. In the Python snippet below, an example of the TTIm Calibrate
317 function is given. It is the same example mentioned in the Fmin optimization above.

```
318
319
320 cal = Calibrate(mlc)
321 cal.parameter(name='kaq0', layer=0, initial=10, pmin=0)
322 cal.parameter(name='kaq1', layer=1, initial=10, pmin=0)
323 cal.parameter(name='Saq0', layer=0, initial=.01, pmin=0, pmax=0.3)
324 cal.parameter(name='Saq1', layer=1, initial=.001, pmin=0, pmax=0.3)
325 cal.parameter(name='res', par=wc.res, initial=0.1)
326 cal.series(name='obs3', x=ro, y=0, layer=[0,1], t=to[mask], h=do[mask])
327 cal.fit()
```

329 These optimization methods require an initial estimate for the parameters. It is possible there is more than
330 one optimal solution which makes the outcome of the optimization dependent on the choice of initial val-
331 ues. Other studies found that T and S values are commonly low in northern Ghana (Owusu et al, 2017).
332 Based on these other studies the following initial conditions are applied: k_{aq0} is 10 (m/d), k_{aq1} is 10 (m/d),
333 S_{aq0} is 0.01 (-), S_{aq1} is 0.001 (-) and well resistance is 0.1 (d). The actual well radius is used as the (initial)
334 borehole storage: 0.0635 (m). Boundary conditions are applied to avoid the optimization resulting in phys-
335 ically improbable parameter values, i.e. negative parameter values and unnaturally high storativity values
336 (greater than 0.3 (-)).

337 2.2. From fieldwork data to T & S values

338 The methods and models mentioned in the previous section are applied on the measurements from the
339 five locations: Bingo, Nungo, Nyong Nayili, Janga and Ziong. A complete overview of all simulations can be
340 found in appendix C. The most important outcomes of this analysis are discussed below for each of the five
341 locations.

342 2.2.1. Location: Bingo

343 Site inspection

344 Sloping landscape, some rocks at surface. Area often struck by bush fires, charred vegetation abundant,
345 agricultural fields not ready for use. Although Volta river not far (on map), no river or ponds seen in direct
346 surroundings. Wet season flooding caused by rain and 'popping up' out ground, labelled as height (1-2m)
347 and disappears in a few days. Well located at walking distance from nearest community. Steel lid, no well
348 screen perforations observed above surface level.

349 350 Measurement quality

351 Start delayed due to malfunctioning power converter. Tangled rope: Position lowest diver undesirably high

352 and hand measurements not completely possible, result: big gap in data. Recovery test started at an early
 353 stage.

354

355 Fit analysis

356 Data points are missing. Total drawdown unknown from a certain moment in time. The analytical (Theis)
 357 solution is not capable of fitting the data. This is most definitely not the case for the data analysed by the use
 358 of TTIm. The use of both parameter optimization methods are capable of dealing with the lack of data. Both
 359 optimizations find optimal parameter values at which drawdown curve exceeds lowest measured ground-
 360 water levels. By this example it is shown it is not by definition required to feature complete drawdown curves
 361 during parameter determination. Even with incomplete drawdown time series it is possible to obtain rea-
 362 sonable fits. Complete overview of all the optimizations applied (13 optimizations in all) can be found in
 363 appendix.. tell about the wobbly curve, due to measured fluctuation in discharge.

364

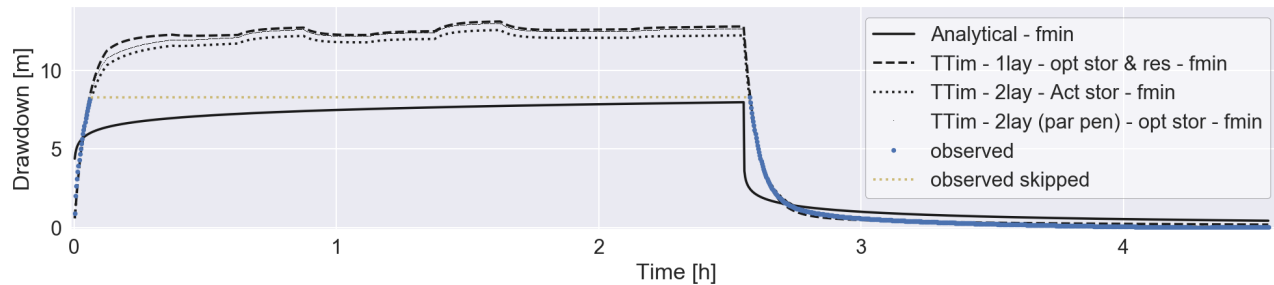


Figure 2.3: Bingo - multi-layer best fits

Table 2.1: Bingo - overview best fit parameters

	Method	Stor [m]	Res [d]	T1	T2 [m^2/d]	S1	S2 [-]	RMSE [m]
Analytical	fmin	-	-	10.83	-	2.0e-04	-	0.798133
1 lay	fmin	0.0647	5.6e-02	26.23	-	6.6e-03	-	0.162757
2 lay	fmin	0.0635	-	2.8e-04	08.25	3.0e-03	2.1e-06	0.107380
2 lay (pp)	fmin	0.0597	-	8.6e-04	07.44	7.1e-03	6.3e-06	0.078188

365 **Final remark** korte uitleg welke fit nou het beste is? en waarom.

366 2.2.2. Location: Nungo

367 **Site inspection**

368 **Measurement quality**

369 **Fit analysis**

370 **Final remark**

371 2.2.3. Location: Nyong Nayili

372 **Site inspection**

373 **Measurement quality** data skip applied. **Fit analysis**

Table 2.2: Nyong Nayili - overview best fit parameters

	Method	Stor [m]	Res [d]	T1	T2 [m^2/d]	S1	S2 [-]	RMSE [m]
Analytical	fmin	-	-	06.00	-	3.0e-01	-	0.751699
1 lay	cal	0.2419	-	13.35	-	7.8e-05	-	0.457474
2 lay	cal	0.2436	-	06.95	06.98	4.6e-06	3.6e-05	0.456774
2 lay (pp)	fmin	0.2659	1.7e-02	1.7e-04	28.61	1.1e-02	4.4e-06	0.450121

374 **Final remark**

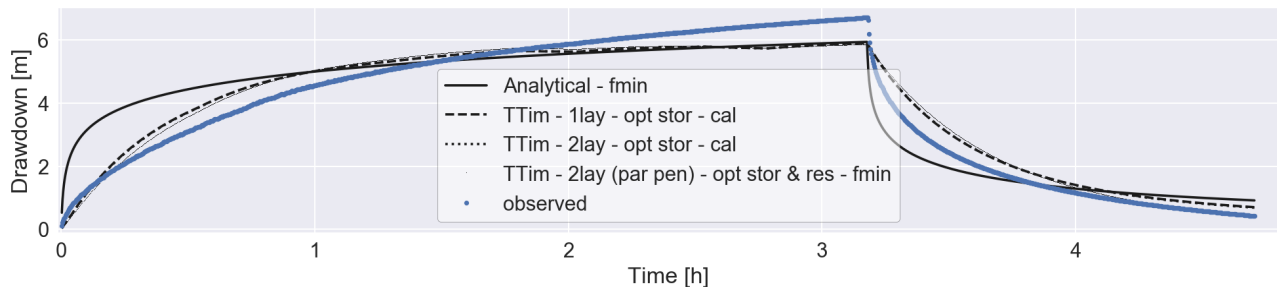


Figure 2.4: Nyong Nayili - multi-layer best fits

375 **2.2.4. Location: Janga (1/2)**

376 **Site inspection**

377 **Measurement quality**

378 **Fit analysis**

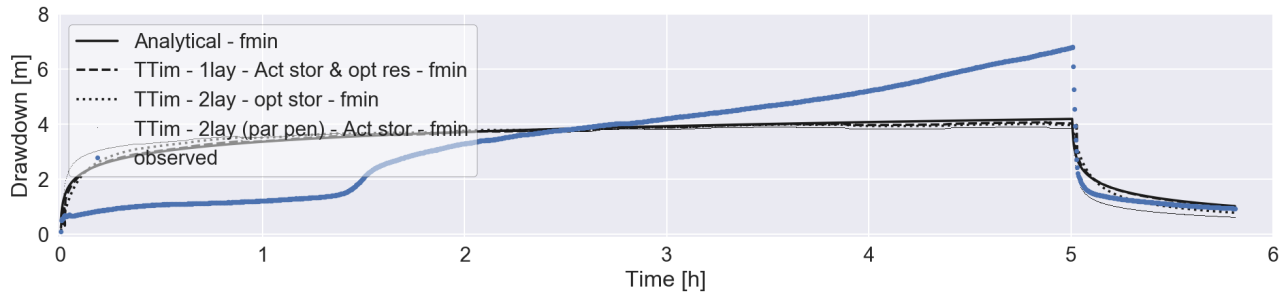


Figure 2.5: Janga first attempt - multi-layer best fits

Table 2.3: Janga first attempt - overview best fit parameters

	Method	Stor [m]	Res [d]	T1	T2 [m²/d]	S1	S2 [-]	RMSE [m]
Analytical	fmin	-	-	08.84	-	3.0e-01	-	1.338604
1 lay	fmin	0.0635	-9.7e-03	09.09	-	1.6e-02	-	1.382181
2 lay	fmin	0.1287	-	12.48	1.3e-04	1.9e-02	1.1e-08	1.444546
2 lay (pp)	fmin	0.0635	-	9.1e-05	15.19	4.3e-08	3.1e-03	1.530254

379 **Final remark**

380 **2.2.5. Location: Janga (2/2)**

381 **Measurement quality**

382 **Fit analysis**

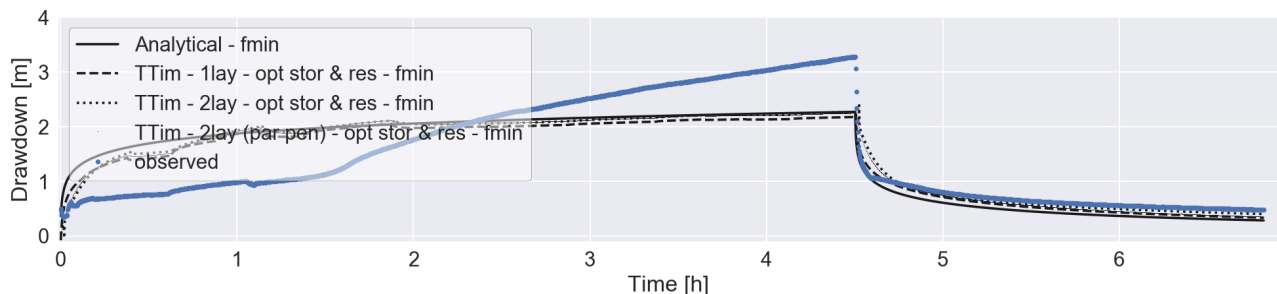


Figure 2.6: Janga second attempt - multi-layer best fits

383 **Final remark**

Table 2.4: Janga second attempt - overview best fit parameters

	Method	Stor [m]	Res [d]	T1	T2 [m ² /d]	S1	S2 [-]	RMSE [m]
Analytical	fmin	-	-	15.97	-	3.0e-01	-	0.570855
1 lay	fmin	5.4e-07	-9.7e-03	13.54	-	1.9e-02	-	0.550853
2 lay	fmin	0.2228	-2.2e-02	02.05	08.13	2.1e-02	4.1e-04	0.544680
2 lay (pp)	fmin	0.2005	-3.1e-02	06.59	00.86	9.4e-05	2.1e-03	0.544540

2.2.6. Location: Ziong (monitoring)

Site inspection

Measurement quality multi day use. Anaytical solution not applied. Fit analysis

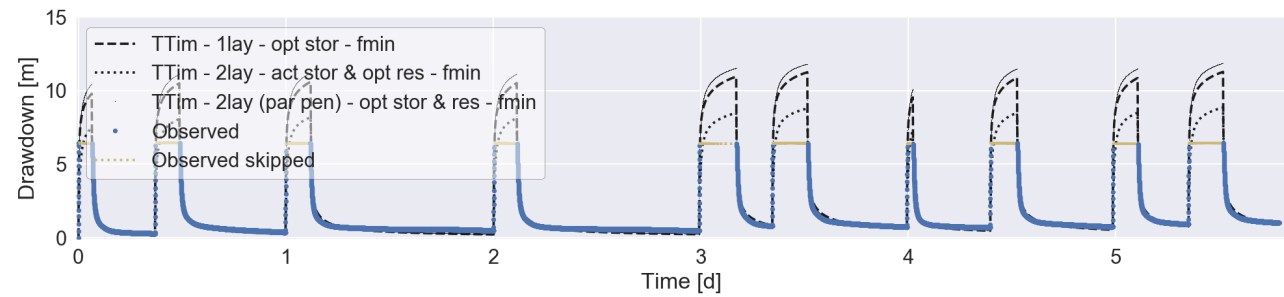


Figure 2.7: Ziong - multi-layer best fits

Table 2.5: Ziong - overview best fit parameters

	Method	Stor [m]	Res [d]	T1	T2 [m ² /d]	S1	S2 [-]	RMSE [m]
1 lay	fmin	0.0382	-	01.76	-	1.1e-03	-	0.254574
2 lay	fmin	0.0635	-0.05	00.38	01.05	2.9e-02	1.2e-03	0.240162
2 lay (pp)	fmin	0.0147	-0.08	00.23	00.78	2.6e-02	1.3e-03	0.243108

Final remark

2.3. Theoretical validation

Soil analysis

VES analysis

2.4. Fieldwork results

summary of the main results Recommendations for further investigation if applicable.

Waardes komen overeen (zelfde range/ordegrootte) met theorie. zoek dit even na

Er is geen duidelijk onderscheid of 1, 2 dan wel 3 laags (partially penetrating) beter dan wel slechter scoort. dus alle schematische gelaagde bodemoppbouw mogelijk.

bespreek hier de tekortkoming van het meten in de well zelf als enige. Werkt gewoon niet heel fijn of nauwkeurig. Voor indicatie wel goed.

vertel over het resultaat van de twee vormen van analyse. fmin versus calibration function. Toch een verschil in algoritme (numerieke solver). Maar resultaten beide slechts tot op zekere hoogte nauwkeurig. Maar dit zal eerder komen door de metingen zelf (in borehole) en de omstansigheden van northern Ghana.

does not happen to often. but if T or S values not in right 'order', it is always assumed highest T values in layer under confining layer (not in lowest layer). based on the known soil type of this layer in borehole logsheet (appendix..).

409 schrijf appendix over de lambda bepaling.

3

410

411

Model scenarios

412 scenario's

413 **3.1. Scenarios**

414 **3.2. Test criteria**

415 **3.3. Run**

416 **3.4. Results & Conclusions**

4

417

418

(Financial) yields - upscaling

419 kostenplaatje

420 **4.1. inhoud**

5

421

422

Conclusions

423 Results short outcome of upscaling. Does it work?

424 Blah blah blah

6

425

426

Discussion & Recommendations

427 good, bad, advice further research

Bibliography

Appendices

429

A

430

431

Original Borehole Logsheets

432 In the first half of the year 2016 Conservation Alliance (CA) commissioned the construction of multiple
433 boreholes in northern Ghana. The boreholes subjected in this research (five locations, visualized in 2.1) are
434 all part of this operation. Valuable information is gained with respect to local soil stratification, during
435 borehole construction. Information is preserved in the original borehole log-sheets, which can be found
436 in this appendix. Besides the local soil stratification, these log-sheets contain information on individual
437 applied well structures. A depth dependent distinction is made in plain versus screened well skin. In terms
438 of content these borehole log-sheets are used as a starting point in the theoretical model determination
439 (section 2.1).

		CONSERVATION ALLIANCE- THE PAVE PROJECT				BH status:	Successful	✓			
						Dry					
BOREHOLE LOG SHEET											
Community		Bingo	District	Talensi	Borehole ID	BH B1					
Coordinates - Latitude (N) : Longitude (W)											
Drilling contractor		Drill rig				Method	ROTARY AIR				
Drilling start date		6-8-2016	Compl. date	6-8-2016	Operator						
TEST PUMPING		Date:		Conductivity		us/cm	Top of screen *	0	m		
Dynamic WL *		m	Pump type	Total Iron		mg/l	Static WL *	m			
Static WL *		m	Pumping rate (Q)	m³/h	Manganese	mg/l	Potential drawdown	m			
Drawdown (s)		m	Duration	h	Nitrate	mg/l	Potential yield	25 l/min			
* Levels to ground level datum		Specific capacity (Q/s)		m³/h/m	Fluoride	mg/l	Depth of borehole *	48	m		
BIT SIZE & TYPE	Temporary Casing	SCALE	PROFILE		TIME/DEPTH M/MIN	WATER ZONES CUMULATIVE Q (l/min)	WELL DIAGRAM				
10"			Light brown clay								
Clay cutter											
6.5" hammer bit			Highly weathered light brown sandstone mixed with shaly materials								
			5					3m PVC Screen			5
			10								10
			15								15
			20								20
			25								25
			30								30
			35								40
			40								45
			45								50
Moderately weathered brownish sandstone					15						
					55						
Remarks and stoppages: Prepared by: Approved: Gravel for gravel pack Screen Length Casing length Installation of grout seal Cleaning & development Centralisers fitted Safety cap fitted Backfill aband. BH Cement for grout Platform construction date Distance from last BH											
Yes		48	LM								
		30	LM								
Yes		18	LM								
		2	M								
Yes		2	HRS								
		No									
Yes		/	No								
			/								
Yes			KG								
Yes			KM								

		CONSERVATION ALLIANCE- THE PAVE PROJECT					BH status:		Successful Dry		✓
		BOREHOLE LOG SHEET					BH N100		BH N100		
Community	Nungo	District	Talensi	Borehole ID	BH N100						
Coordinates - Latitude (N) :		Longitude (W)									
Drilling contractor		Drill rig			Method	ROTARY AIR					
Drilling start date	6-8-2016	Compl. date	6-8-2016		Operator	Kwaku					
TEST PUMPING		Date:		Conductivity	us/cm	Top of screen *	0	m			
Dynamical WL *	m	Pump type		Total Iron	mg/l	Static WL *		m			
Static WL *	m	Pumping rate (Q)	m³/h	Manganese	mg/l	Potential drawdown		m			
Drawdown (s)	m	Duration	h	Nitrate	mg/l	Potential yield	80 l/min				
* Levels to ground level datum		Specific capacity (Q/s)	m³/h/m	Fluoride	mg/l	Depth of borehole *	42	m			
BIT SIZE & TYPE	Temporary Casing Scale	PROFILE			TIME/DEPTH M/MIN	WATER ZONES CUMULATIVE Q (l/min)	WELL DIAGRAM				
10"		Highly weathered light brown sandstone									
Clay cutter		5									
6.5"		10									
hammer bit		15	Moderately weathered light grey sandstone mixed with shaly materials (at 18m, 21-24m)								
		20									
		25									
		30									
		35	Light grey sandstone				55				
		40									
		45					80				
		50									
Gravel for gravel pack		42	LM	Remarks and stoppages:							
Screen Length		36	LM								
Casing length		6	LM								
Installation of grout seal		M									
Cleaning & development		2	HRS	Prepared by:							
Centralisers fitted		No									
Safety cap fitted	Yes	/	No	Approved:							
Backfill aband. BH	Yes	No	/								
Cement for grout			KG								
Platform construction date			KM								
Distance from last BH											

		CONSERVATION ALLIANCE- THE PAVE PROJECT				BH status:		Successful Dry	
		BOREHOLE LOG SHEET				BH NN1		Kwaku	
Community	Nyong Nayili	District	Karaga	Borehole ID	BH NN1				
Coordinates - Latitude (N) : Longitude (W)									
Drilling contractor		Drill rig			Method	ROTARY AIR			
Drilling start date	31/05/2016	Compl. date	31/05/2016	Operator	Kwaku				
TEST PUMPING		Date:		Conductivity	us/cm	Top of screen *	0	m	
Dynamic WL *	m	Pump type		Total Iron	mg/l	Static WL *		m	
Static WL *	m	Pumping rate (Q)		Manganese	mg/l	Potential drawdown		m	
Drawdown (s)	m	Duration		Nitrate	mg/l	Potential yield			
* Levels to ground level datum		Specific capacity (Q/s)		Fluoride	mg/l	Depth of borehole *	54	m	
BIT SIZE & TYPE	Temporary CASING SCALE	PROFILE		TIME/DEPTH M/MIN	WATER ZONES CUMULATIVE Q (l/min)	WELL DIAGRAM			
10"									
Clay cutter		Clay							
	5								
6.5"									
hammer bit									
	10								
	15								
	20	Highly weathered chocolate brown sandstone							
	25								
	30								
	35								
	40								
	45	Moderately weathered chocolate brown sandstone							
	50								
	55								
Gravel for gravel pack		54	LM	Remarks and stoppages:					
Screen Length		33	LM						
Casing length		21	LM						
Installation of grout seal		M							
Cleaning & development		2	HRS	Prepared by:					
Centralisers fitted		No							
Safety cap fitted	Yes	/	No	Approved:					
Backfill aband. BH	Yes		No						
Cement for grout			/						
Platform construction date			KG						
Distance from last BH			KM						

		CONSERVATION ALLIANCE- THE PAVE PROJECT				BH status:	Successful	✓	
						Dry			
BOREHOLE LOG SHEET									
Community		Janga 1	District	West Mamprusi	Borehole ID	BH J1			
Coordinates - Latitude (N) :		0°iu	Longitude (W)						
Drilling contractor			Drill rig		Method	ROTARY AIR			
Drilling start date		6-3-2016	Compl. date	6-3-2016	Operator	Kwaku			
TEST PUMPING		Date:		Conductivity	us/cm	Top of screen *	0	m	
Dynamic WL *		m	Pump type	Total Iron	mg/l	Static WL *		m	
Static WL *		m	Pumping rate (Q)	m³/h	Manganese	mg/l	Potential drawdown	m	
Drawdown (s)		m	Duration	h	Nitrate	mg/l	Potential yield	35 l/min	
* Levels to ground level datum			Specific capacity (Q/s)	m³/h/m	Fluoride	mg/l	Depth of borehole *	48 m	
BIT SIZE & TYPE	Temporary Casing	SCALE	PROFILE	TIME/DEPTH M/MIN	WATER ZONES CUMULATIVE Q (l/min)	WELL DIAGRAM			
10" Clay cutter	6.5" hammer bit		Highly weathered light brown sandstone (Very loose formation) Moderately weathered grey shale		15 35				
						5			
						10			
						15			
						20			
						25			
						30			
						35			
						40			
						45			
50									
Gravel for gravel pack		Yes	48	LM	Remarks and stoppages:				
Screen Length			48	LM					
Casing length				LM					
Installation of grout seal				M					
Cleaning & development			2	HRS	Prepared by:				
Centralisers fitted				No					
Safety cap fitted			/	No	Approved:				
Backfill aband. BH				/					
Cement for grout				KG					
Platform construction date									
Distance from last BH			KM						

		CONSERVATION ALLIANCE- THE PAVE PROJECT				BH status:	Successful	✓		
						Dry				
BOREHOLE LOG SHEET										
Community	Ziong	District	Savelugu Nanton	Borehole ID	BH Z1					
Coordinates - Latitude (N) : Longitude (W)										
Drilling contractor		Drill rig		Method	ROTARY AIR					
Drilling start date	27/05/2016	Compl. date	27/05/2016	Operator						
TEST PUMPING		Date:		Conductivity	us/cm	Top of screen *	0	m		
Dynamic WL *	m	Pump type		Total Iron	mg/l	Static WL *		m		
Static WL *	m	Pumping rate (Q)		m³/h	Manganese	mg/l	Potential drawdown	m		
Drawdown (s)	m	Duration		h	Nitrate	mg/l	Potential yield	25 l/min		
* Levels to ground level datum		Specific capacity (Q/s)		m³/h/m	Fluoride	mg/l	Depth of borehole *	48 m		
BIT SIZE & TYPE	Temporary Casing	PROFILE SCALE	TIME/DEPTH M/MIN	WATER ZONES CUMULATIVE Q (l/min)	WELL DIAGRAM					
10"										
Clay cutter										
6.5" hammer bit		Reddish brown laterite								
		5								
		10								
		15								
		20								
		25								
		30								
		35								
		40								
		45								
50										
Highly weathered light brown sandstone mixed with shaly materials										
Moderately weathered brownish sandstone										
15										
25										
3m PVC Screen										
12m PVC Plain										
48m Gravel pack										
33m PVC Screen										
1m Bail Plug										
50										
Gravel for gravel pack	Yes	48	LM	Remarks and stoppages:						
Screen Length		36	LM							
Casing length		12	LM							
Installation of grout seal		M	HRS							
Cleaning & development		2	HRS	Prepared by:						
Centralisers fitted		No								
Safety cap fitted		/	No	Approved:						
Backfill aband. BH		Yes	/							
Cement for grout			KG							
Platform construction date			KM							
Distance from last BH										

B

445

446

Fieldwork set-up

447 The northern Ghana in-field geohydrological data collection would not have been possible without the in-
448 terference of Conservation Alliance (CA). Spread over the Upper East and Northern Region the NGO holds
449 multiple PIT locations. Five locations, visible in figure 2.1, are appointed as measurement locations for the
450 purposes of this research. Besides the research locations, CA provided transport, an interpreter and pump-
451 ing test equipment. The section below contains detailed information on the equipment applied. Moreover,
452 it describes the general fieldwork pumping test / monitoring set-up. The section concludes with fieldwork
453 fact-sheets, containing the collected data for each individual location.

454 **B.1. Equipment**

455 The applied in-field pumping tests are executed with a same set of equipment. The paragraph below con-
456 tains a detailed description of the most important tools. In this case a distinction has been made between
457 the equipment for the pumping tests and the actual groundwater measurements. Moreover small equip-
458 ment as pliers, screwdrivers, gloves and robes are ignored. Purposes and use of these tools are taken for
459 granted.

460

461 **Pumping test**

- 462 • Pump: Pedrollo 4" submersible pump; Type 4SR4/18

463 A 2 HP pump, for example usable for the supply of water to irrigation fields. While pumping the water
464 should preferably not exceed 35 °C and should not contain too many particles; no more than 150
465 g/m³. The pump can be submerged in water up to 100 meters. Installed in the right way, the pump
466 can deliver 20-100 l/min with an head difference of 112-45 m. More specific information regarding
467 the pump can be found on the Pedrollo webpage.



Figure B.1: Comparable example of the fieldwork submersible pump
(source: <https://www.pedrollo.com/en/4sr-4-submersible-pumps/150>)

468 • Generator & power converter: Kipor diesel generator - 5 kVA
 469 A mobile generator has been used as a pump power source. The Kipor generator is a relatively small
 470 model, easy to handle and meets the pump requirements by the use of the 230 V connection. A power
 471 converter is placed between generator and pump to manually switch on and off the pump. To facili-
 472 tate a flawless transfer between generator and pump one should be aware the cables and connections
 473 towards the pump should be waterproof. Moreover these power cables should be of a decent length
 474 to allow the pump to submerge.



Figure B.2: Comparable example of the fieldwork generator
 (source: <https://www.kipor-power.eu/winkel/kipor-kde6700t-diesel-generator-5-kva/>)

475 • Hose:

476 As a transport line towards the location of discharge a flexible water hose has been attached to the
 477 pump. The hose has been manufactured in Polyethylene, has an external diameter of $1\frac{1}{4}$ " and is
 478 approximately 100 m long.



Figure B.3: Actual fieldwork hose & bucket

479 • Bucket:

480 As a rough estimation for discharge an plastic bucket has been used. This oversized measuring cup
 481 stores volumes up to 50 l and contains 5 l level indicators.

482 **GWT measurements**

483 • Pressure sensor data loggers:

484 - Van Essen; TD-Diver Type DI801 (2x) & Baro-Diver Type DI800 (1x):

485 TD- and Baro-Divers are applied for the measuring and recording of time dependent fluctuations in
 486 (ground)water levels, atmospheric pressures and temperatures. The TD-Divers can record a water
 487 column up to 10 m. Baro-Divers can be used to measure atmospheric pressures and shallow water
 488 levels, approximately up to a range of 0.9 m. Based on the internal memory these devices can store

489 up to 72.000 measurements per parameter. Measurement logging can be programmed by the use
 490 of a USB-Unit and the Diver-Office software. With a battery life of 10 years, long and/or short term
 491 measurements can be applied with a sample interval of 0.5 seconds to 99 hours. Moreover the sample
 492 interval can be linear or logarithmic.



Figure B.4: Comparable examples of Van Essen TD- & Baro-Divers
 (source: <https://www.vanessen.com/images/PDFs/TD-Diver-DI8xx-ProductManual-nl.pdf>)

493 - In-Situ; RuggedTROLL100 (2x) & BaroTROLL (1x):

494 Rugged TROLL 100 and BaroTROLL divers are applied for the measuring and recording of time depen-
 495 dent fluctuations in (ground)water levels, atmospheric pressures and temperatures. The RuggedTROLL100
 496 divers function in a pressure range up to 9 m water column. BaroTROLL divers can be used for the
 497 measurement of atmospheric pressures, up to 1 bar. The internal memory of 2.0 MB accommodates
 498 the storage of 120.000 data records. A record contains a set of three items; date & time, pressure and
 499 temperature. The internal battery has a lifetime of approximately 10 years. By the use of the Rugged
 500 TROLL docking-station and the Win-Situ 5 software, linear logging can be programmed. Fastest log-
 501 ging rate is 1 log per second for the Rugged TROLL 100 divers and 1 log per minute for the BaroTROLL
 502 divers. Optionally it is possible to display the pressure in units of Psi, Bar, Pascal or mH₂O.



Figure B.5: Comparable examples of In-Situ TD- & Baro-Divers
 (source: <https://in-situ.com/product-category/water-level-monitoring/level-temp-data-loggers/>)

503 • Hand measurement device: Heron water tape

504 The water tape is applied to hand measure static water levels and verify drawdown water levels during
 505 the pumping tests. The water tape has a length of 300 ft (100 m). A water level sensing probe is
 506 attached to the tail of the tape. Probe water contact results in an instant auditory signal, after which
 507 the depth can be determined by eye. Product specifications can be found on the Heron webpage.

508 **B.2. General measurement structure**

509 This section accommodates multiple key aspects in the test set-up. By the implementation of this thought-
 510 out pumping test and measurement set-up an optimal test result is pursued. Moreover it accommodates



Figure B.6: Comparable example of the fieldwork water tape
 (source: <https://envirotechonline.com/water-level-interface-meters/the-heron-water-tape.html>)

511 information on fieldwork reproduction.

512 **Pump installation**

513 Based on the log sheets the original (2016) site-specific borehole depths are known in advance. Due to the
 514 accumulation of sedimentation the borehole depth decreases over time. To prevent pump damage and
 515 make sure proper functioning is maintained, the actual borehole depths are measured before the pump-
 516 ing tests. Outcome of the measurements are taken into account for each individual test set-up. To prevent
 517 excessive spread of soil particles the submersible pump is positioned at least 5 meters above the measured
 518 bottom. In practice this resulted in a pump suction depth of approximately 35 m for every individual pump-
 519 ing test.

520 **Discharge (measurement)**

521 A single 100 m hose is directly connected to the outlet of the submersible pump. Based on the pump pos-
 522 ition (deep inside borehole), a length of circa 60 m is still present for the horizontal displacement of water.
 523 At this distance (relative to the borehole) water is discharged on the surface.
 524 The head of the hose is equipped with a nozzle to roughly regulate the discharge rate. By the use of this noz-
 525 zle, discharge rates in the range of 50-75 m³/d are obtained during the pumping tests. Rates are measured
 526 by the use of a 50 l bucket. Starting at the moment of pump operation, the duration of filling is measured
 527 twice every 15 minutes. The average is used to calculate the time dependent discharge rates. More detailed
 528 discharge information can be found in the site-specific fact-sheets below.

529 **GWT measurement**

530 Drawdowns due to pumping tests are preferably measured in multiple piezometers located at a certain
 531 known horizontal distance from the discharge well (Kruseman & de Ridder, 2000). In the northern Ghana
 532 surroundings, close range monitoring options are absent. Due to a lack of time and/or resources these fa-
 533 cilities cannot be arranged either. Moreover, the implementation of such facilities do not match research
 534 nature. Aim of this research is to collect fieldwork data by the use of minimal resources. The local absence of
 535 abundant measurement options strengthens this approach. In this research pumping test GWT drawdowns
 536 are measured in the discharge well only.

537 A water tape (hand equipment) is used, first of all to determine the initial (static) GWT. Subsequently the de-
 538 vice is applied as a real time indicator of drawdown. During the pumping test multiple hand measurements
 539 are applied at randomly picked moments to monitor test progress. Gathered data functions as verification
 540 and back-up of the pressure sensors, which are normative.

541 Two types of divers (different brands) are used as basic GWT measurement devices. Specifications show
 542 these divers can respectively measure pressures up to 10 m (Van Essen) and 9 m (In-Situ) water column
 543 (bron.). The northern Ghana regional subsurface is characterized as highly heterogeneous. The pumping
 544 test GWT drawdown order of magnitude is therefore unpredictable. To prevent the occurrence of missing

545 drawdown data, the single borehole accommodates multiple divers at ascending depths. The water column
 546 between the initial static water table and pump position is preferably filled with about four divers, with a
 547 mutual distance that meets the divers range specifications. To make sure the divers stay in position they are
 548 leashed to a rope which runs from well top to pump. This measurement set-up forms a robust network for
 549 the collection of drawdown data.

550 Practical circumstance can however cause the application of a more simplified set-up. One can think of a
 551 situation in which the pump is already installed and/or will not be removed at the end of the pumping test.
 552 Rope attachment of the divers to the pump is in this case no longer possible. Adverse effect of the sim-
 553 plified set-up is a data collection which is more vulnerable. To prevent the occurrence of undesired diver
 554 movement a minimum distance of 5-10 m between pump and lowest diver is implemented in the simplified
 555 set-up. A complete overview of the borehole measurement set-up (desired and simplified) can be found in
 556 figure B.7.

557

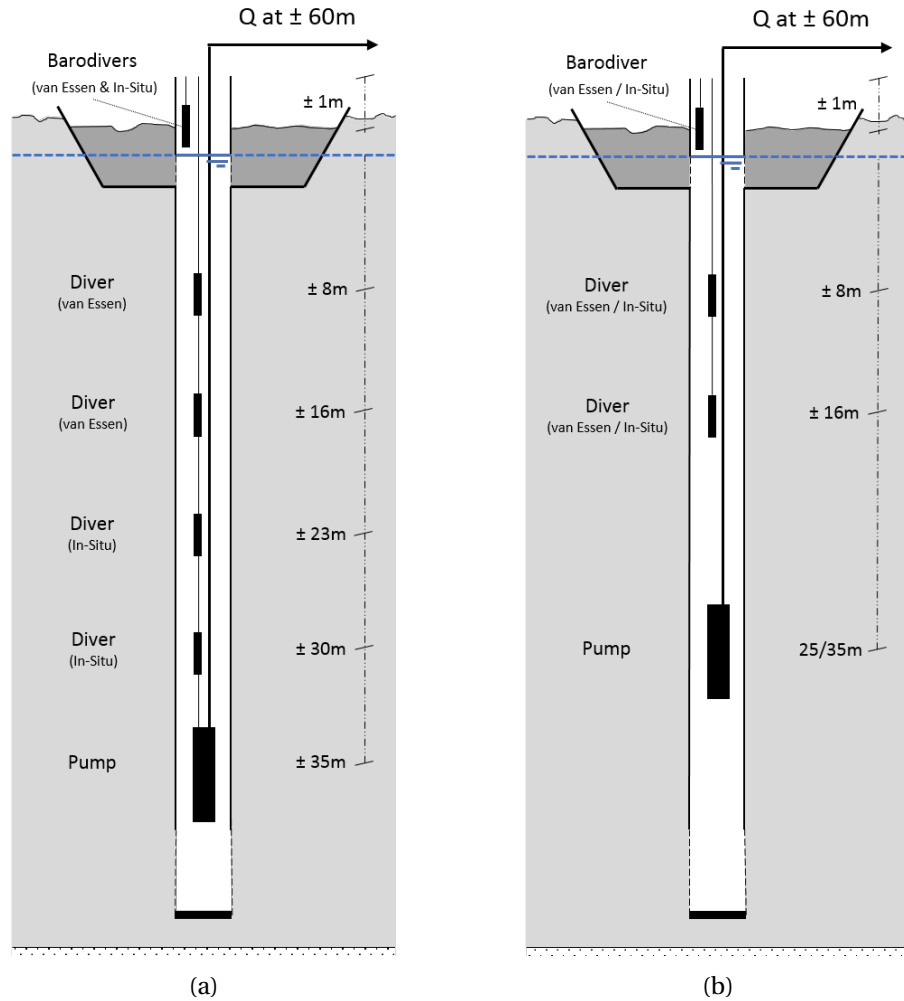


Figure B.7: Fieldwork (measurement) set-up (a) general, (b) simplified

558 Besides the divers the measurement set-up also accommodates two Baro-divers (van Essen & In-Situ), posi-
 559 tioned in the borehole top section. Drawdown is by definition expressed as time dependent GWT reductions
 560 relative to the initial status (bron.). Short term atmospheric fluctuations in pressure are compared to the
 561 water pressures negligible small. Nonetheless these minor atmospheric influences are also included in the
 562 data collection. The inclusion of these Baro-diver measurements increases measurement accuracy, espe-
 563 cially with respect to the multi-day system monitoring.

564 The exact start of pump operation could not be determined in advance. To avoid unnecessary risks in miss-
 565 ing out on the collection of drawdown data, all pressure sensors are programmed to start logging well in
 566 time (08:00:00, local time, at pumping test days). All divers are set to log with a similar linear interval of

567 10 seconds. Only exception is the In-Situ BaroTROLL, which is programmed to linear log at its minimum
568 sample interval; once a minute.

569 **B.3. Site-specific measurement results**

570 In consultation with Conservation Alliance (CA), a total of five pumping tests are applied in boreholes lo-
571 cated at Bingo, Nungo, Nyong Nayili and Janga. By the use of a fifth borehole, location Ziong, the day-to-day
572 PIT system-use is monitored for a week. All tests are applied in November-December 2017, shortly after the
573 transition from wet to dry season. Geohydrological data is gathered by the application of the general pump-
574 ing test set-up (as described above) at the location Nungo, Nyong Nayili and Janga. The simplified set-up is
575 applied at the location Bingo and Ziong. Outcome of the tests are widespread. Detailed site-specific results
576 are displayed in the fact-sheet figures below (Figures B.8 - B.13).

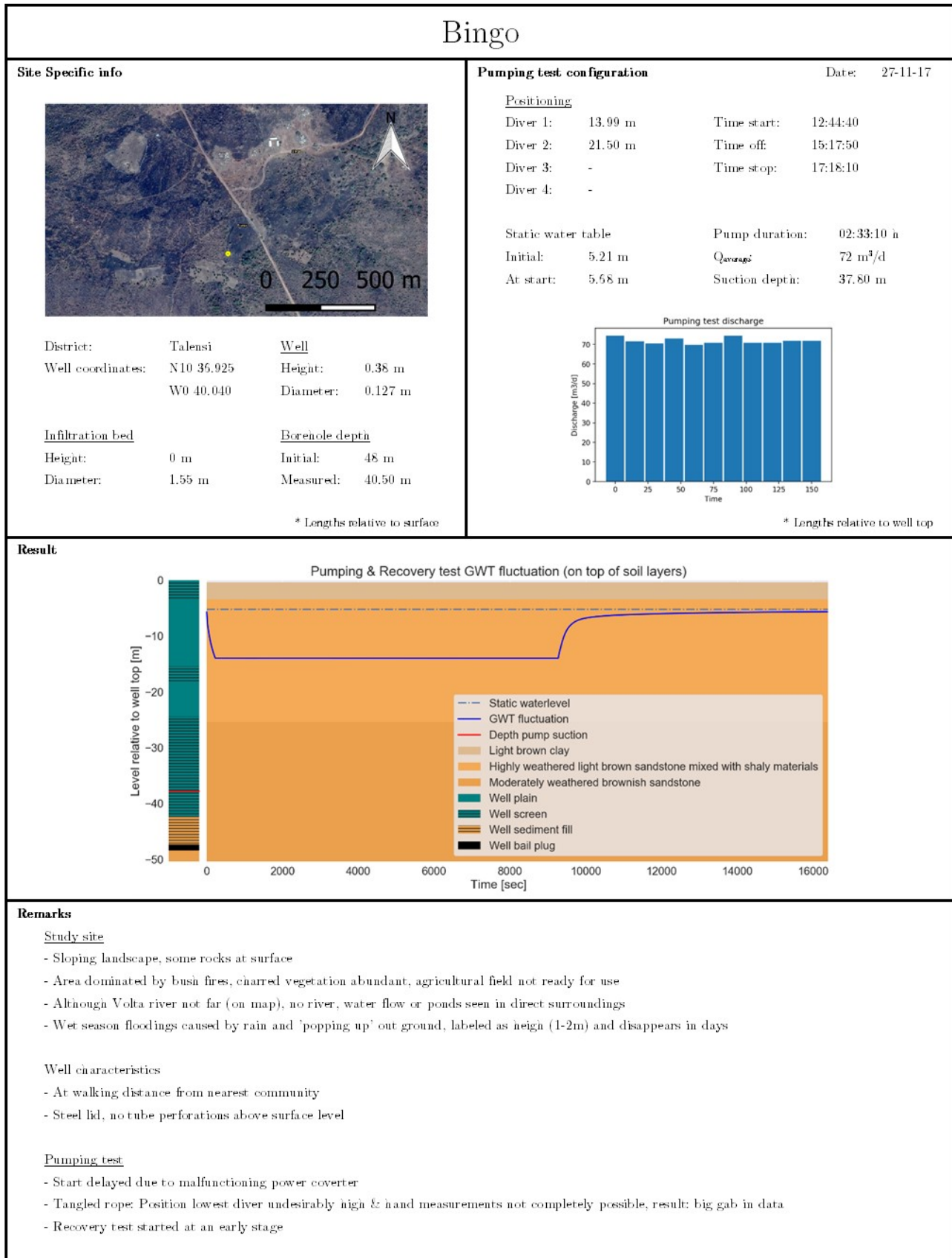


Figure B.8: Fieldwork fact-sheet: Bingo

Nungo		
Site Specific info	Pumping test configuration	Date: 28-11-17
 <p>District: Tafensi Well</p> <p>Well coordinates: N10 33.419 Height: 0.51 m W0 38.990 Diameter: 0.127 m</p>	<u>Positioning</u> Diver 1: 9.05 m Time start: 09:45:00 Diver 2: 17.90 m Time off: 11:00:00 Diver 3: 26.05 m Time stop: 11:15:00 Diver 4: -	
	<u>Static water table</u> Initial: 3.02 m Pump duration: 01:15:00 h At start: 3.00 m Q _{average} : < 5 m ³ /d Suction depth: 31.20 m	
		Pumping test aborted
<u>Infiltration bed</u> Height: -0.35 m Initial: 42 m Diameter: 1.50 m Measured: 9.80 m		
		* Lengths relative to surface
		* Lengths relative to well top
Result -		
		Pumping test aborted
Remarks		
<u>Study site</u> - Mildly sloped till flat landscape - Vegetation abundant, agricultural field present but not ready for use - Volta river in close range (approximately 400 m) - Wet season floodings caused by riverbank overtopping; labeled as extreme (>3m) and constant; duration as long as wetseason		
<u>Well characteristics</u> - At short walking distance from nearest community - No lid, and tube perforations present above surface level		
<u>Pumping test</u> - Pump hard to descend in well; well clogged due to combination of clay, sand and water - Discharge rates very low during test - To improve discharge, test multiple times applied with increased position of pump suction - No drawdowns perceived, pumping test aborted		

Figure B.9: Fieldwork fact-sheet: Nungo

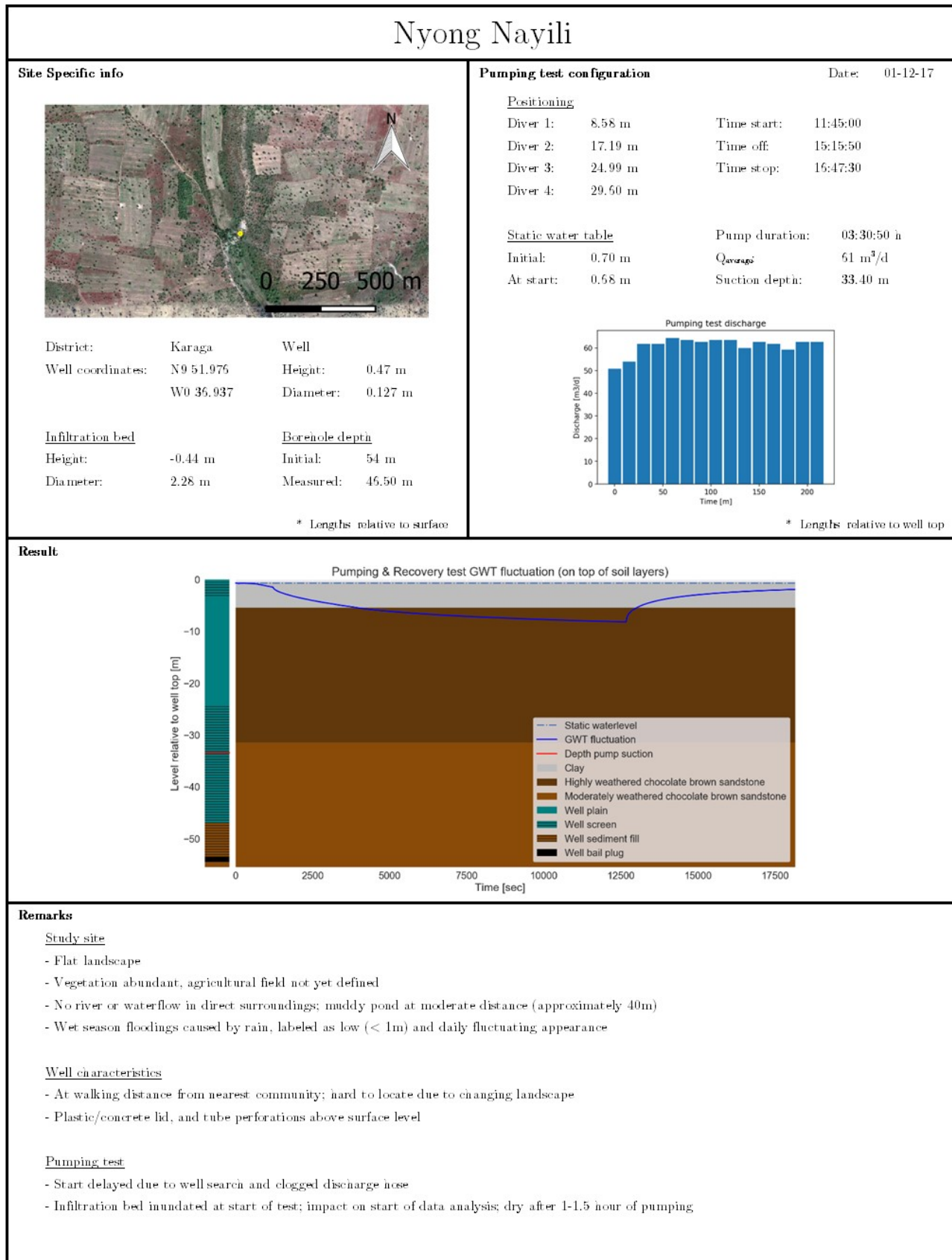


Figure B.10: Fieldwork fact-sheet: Nyong Nayili

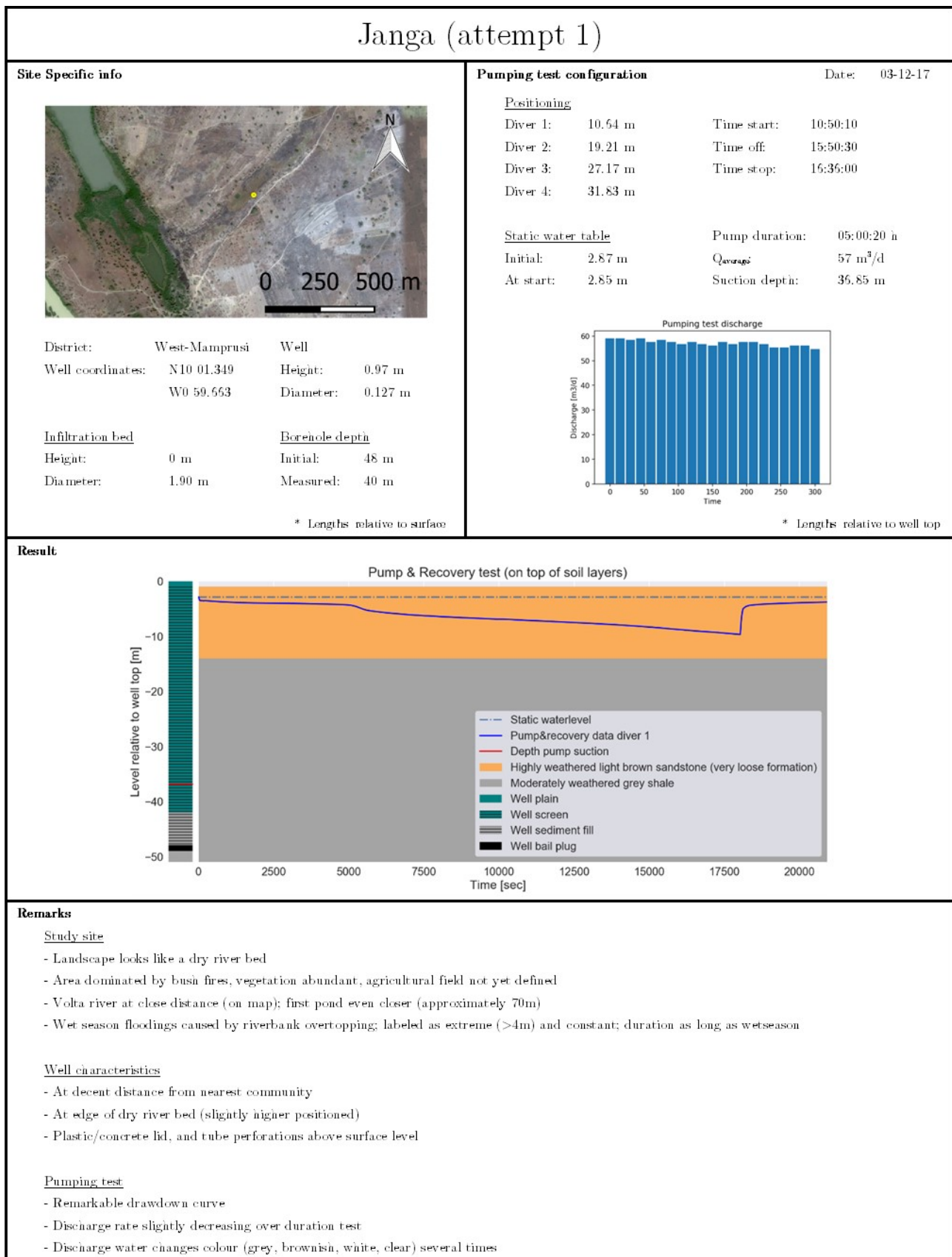


Figure B.11: Fieldwork fact-sheet: Janga (attempt 1)

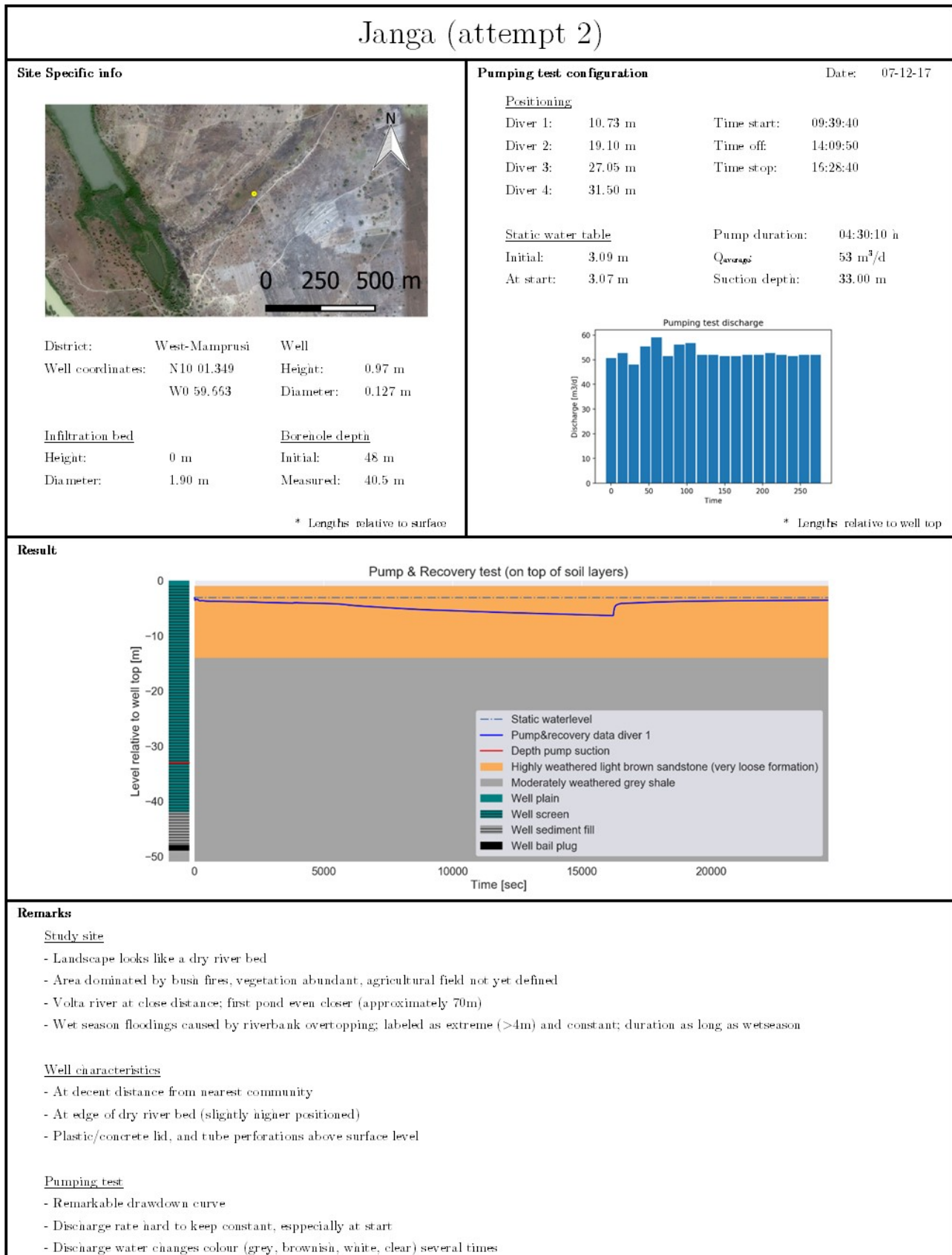


Figure B.12: Fieldwork fact-sheet: Jamga (attempt 2)

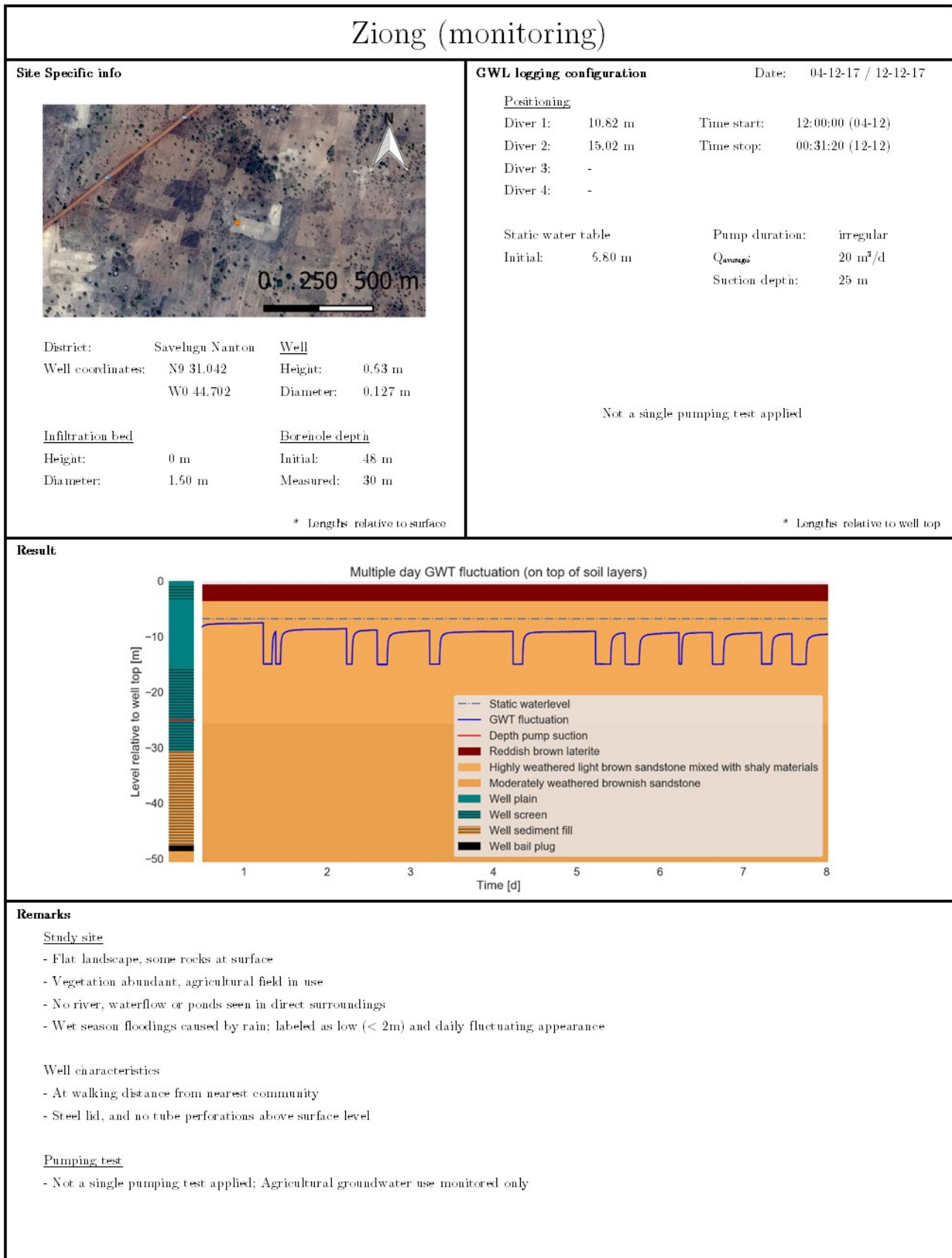


Figure B.13: Fieldwork fact-sheet: Ziong (location of monitoring)

C

577

578

Extense report - Fieldwork data analysis

579 This appendix accommodates a complete overview in fieldwork data analysis. Each location specific dataset
580 is analysed by a distinction in method (analytical Theis's method (single layer), Fmin-RMSE and TTIm Cal-
581ibrate) and theoretical model (single layer, double layer, partially penetrating double layer). In the TTIm
582 analysis an additional distinction is made between analysis by the use of (a) actual borehole storage and no
583 well resistance, (b) optimal borehole storage and no well resistance, (c) actual borehole storage and opti-
584 mal well resistance, (d) optimal borehole storage and optimal well resistance. Result is the location specific
585 dataset analysis subjected to 25 different approaches; analytical (1x), Fmin-RMSE (4x3 = 12x) and TTIm Cal-
586ibrate (4x3 = 12x). Outcomes in geohydrological parameter values can be found in the tables and figures
587 below.

588 C.1. Bingo - overview

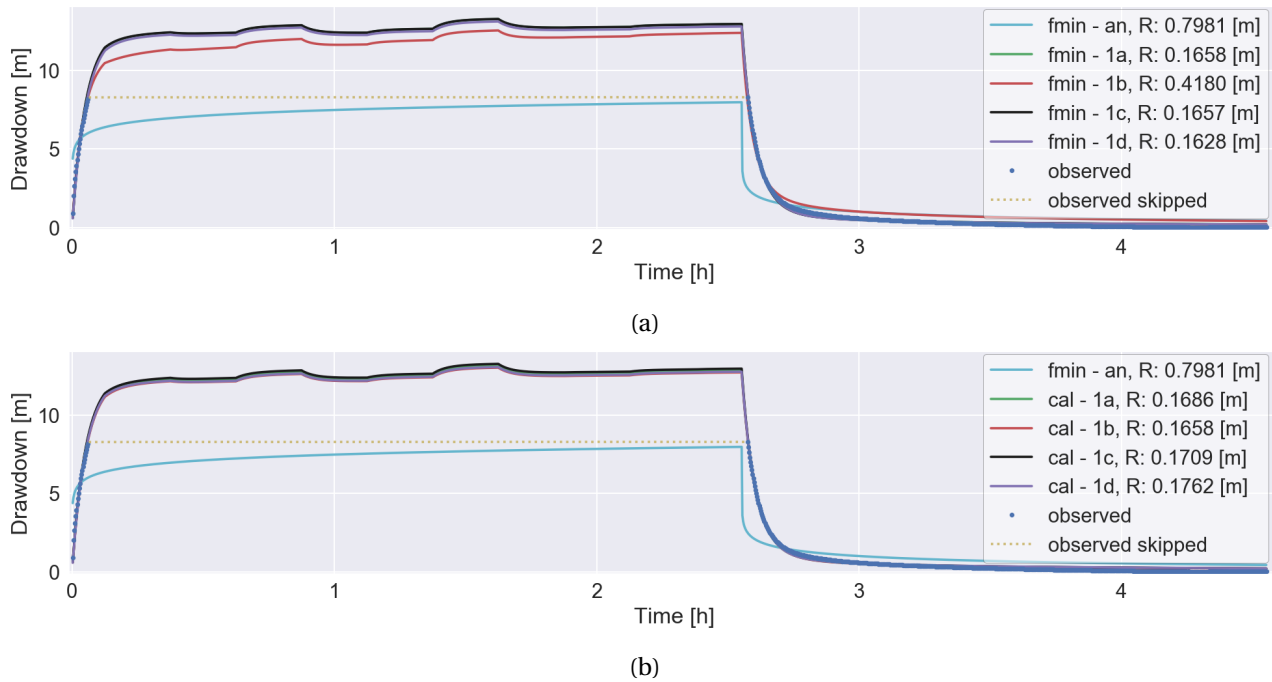


Figure C.1: Bingo single layer fieldwork data analysis by the optimization (a) fmin-RMSE method and (b) TTIm calibration method

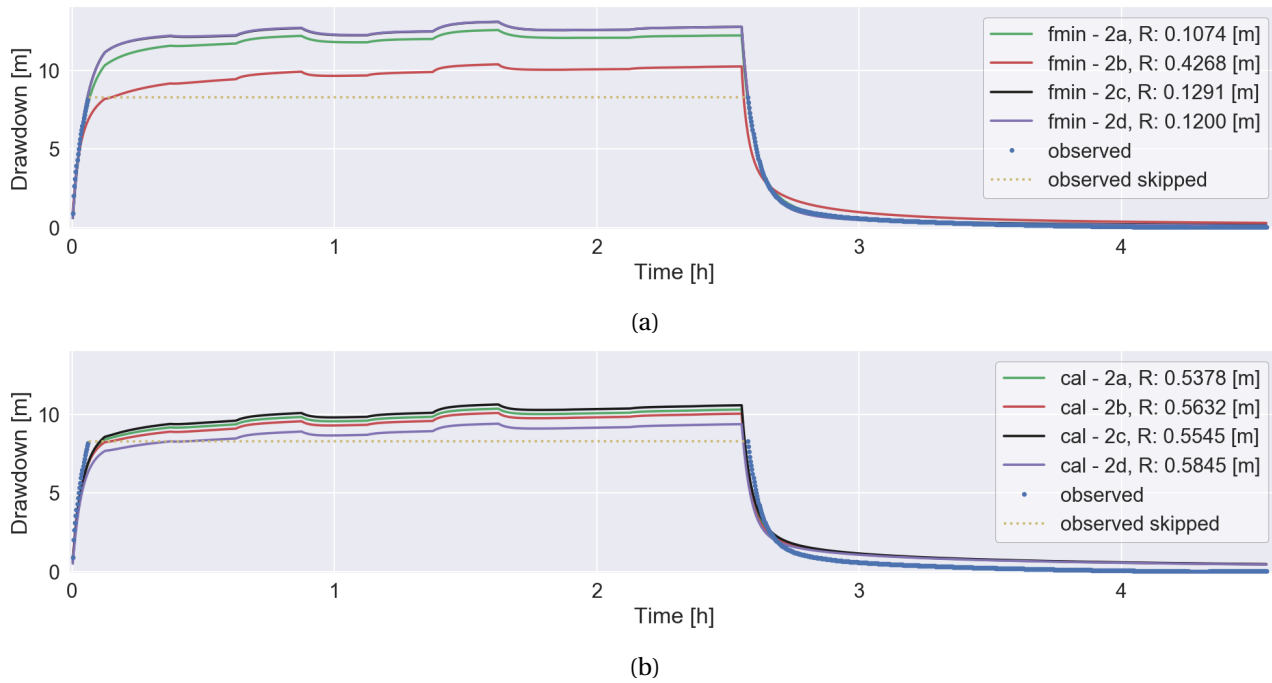


Figure C.2: Bingo double layer fieldwork data analysis by the optimization (a) fmin-RMSE method and (b) TTIm calibration method

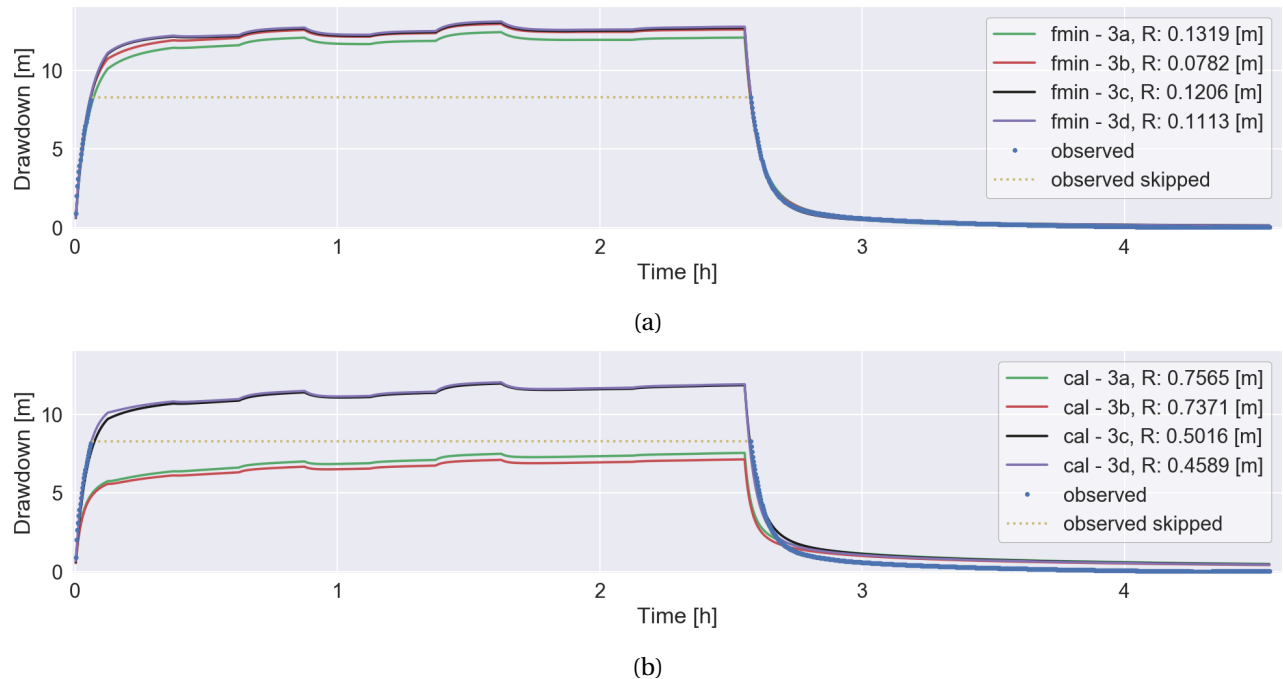


Figure C.3: Bingo partially penetrating double layer fieldwork data analysis by the optimization (a) fmin-RMSE method and (b) TTim calibration method

589 **C.2. Nungo - overview**

590 Gained fieldwork data at the location Nungo not sufficient for the analysis of geohydrological parameter
591 values.

592 **C.3. Nyong Nayili - overview**

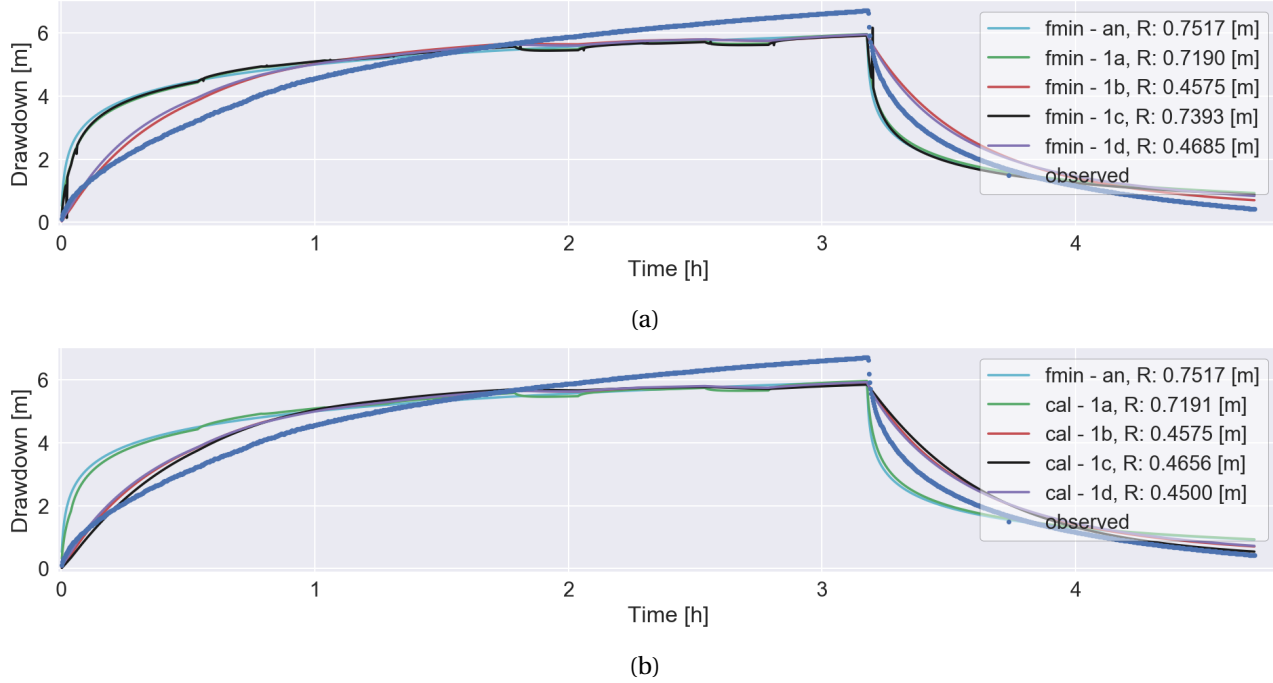


Figure C.4: Nyong Nayili single layer fieldwork data analysis by the optimization (a) fmin-RMSE method and (b) TTIm calibration method

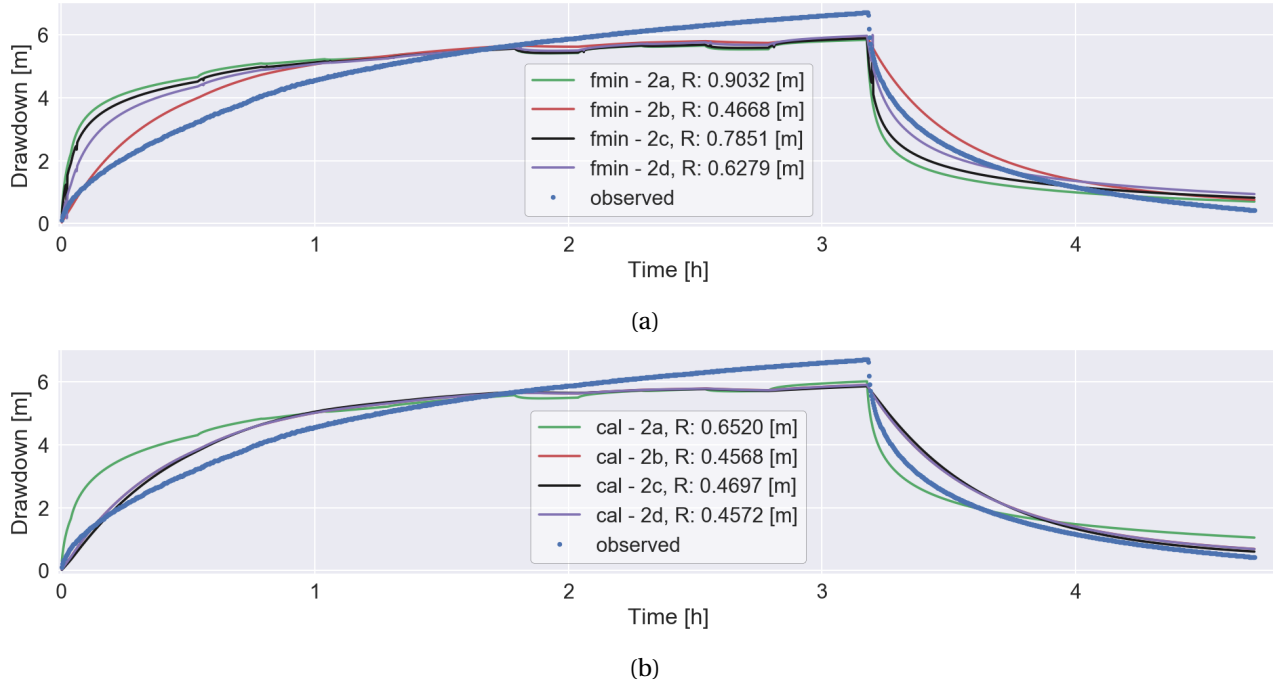


Figure C.5: Nyong Nayili double layer fieldwork data analysis by the optimization (a) fmin-RMSE method and (b) TTIm calibration method

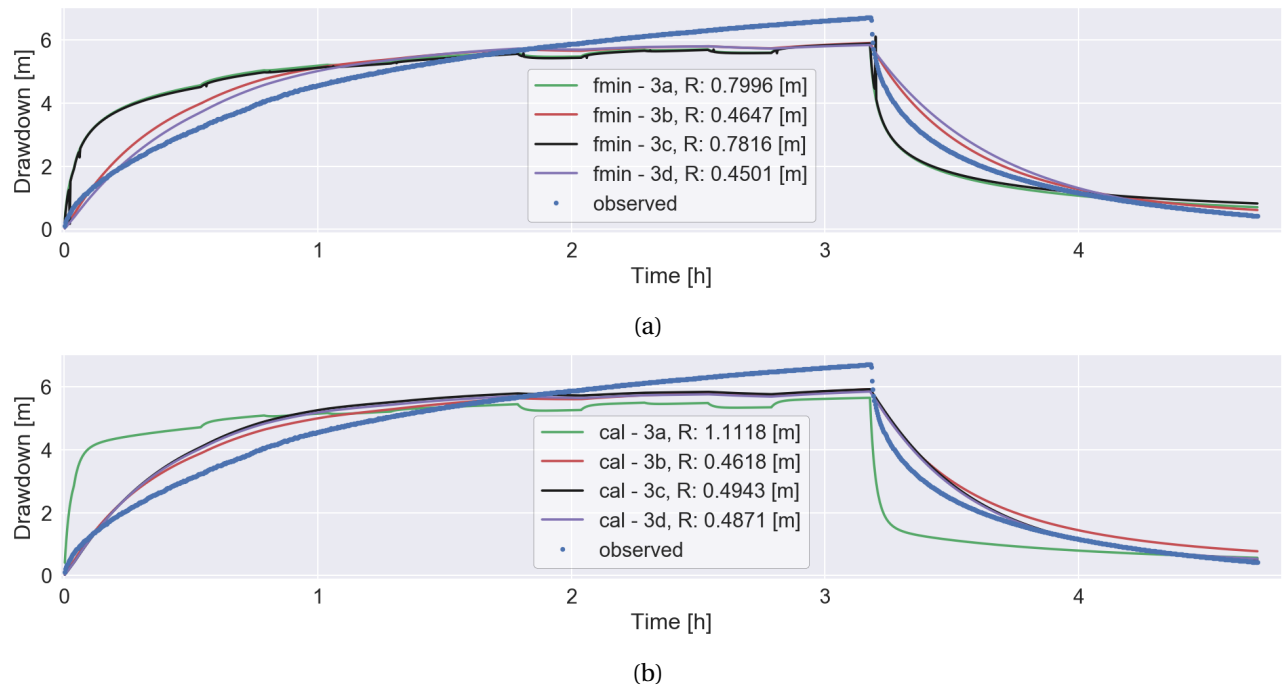


Figure C.6: Nyong Nayili partially penetrating double layer fieldwork data analysis by the optimization (a) fmin-RMSE method and (b) TTIm calibration method

593 **C.4. Janga first attempt - overview**

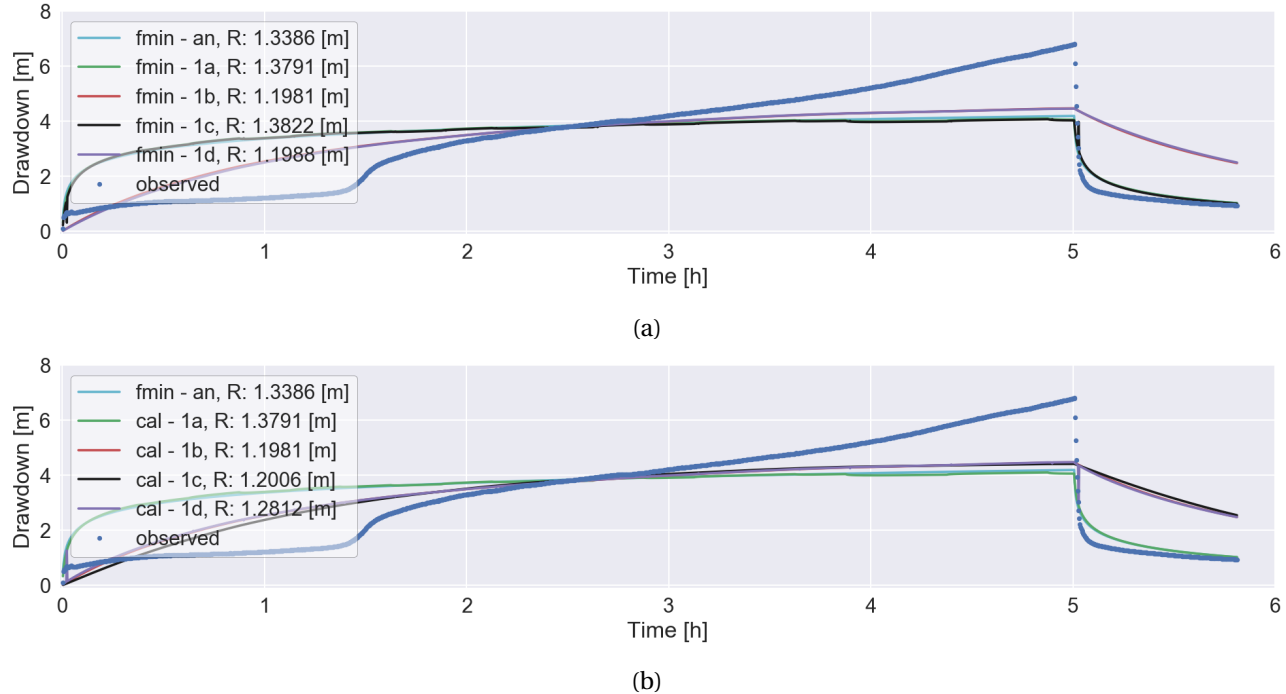


Figure C.7: Janga first attempt single layer fieldwork data analysis by the optimization (a) fmin-RMSE method and (b) TTIm calibration method

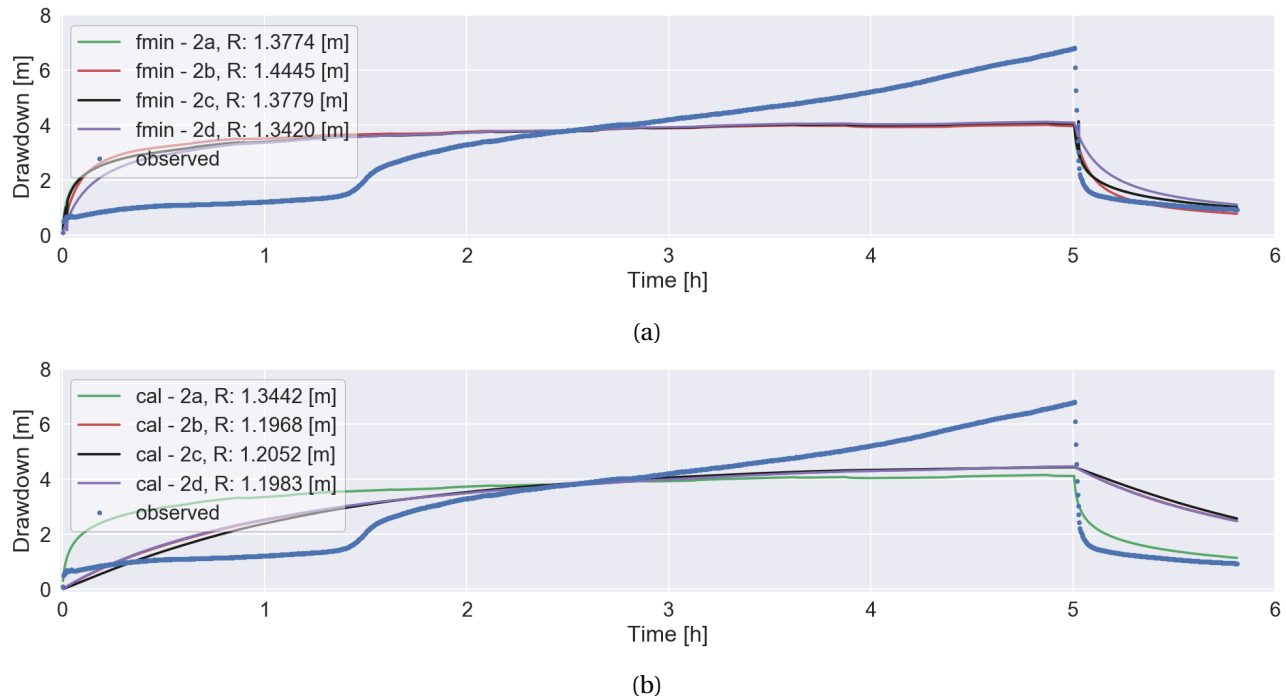


Figure C.8: Janga first attempt double layer fieldwork data analysis by the optimization (a) fmin-RMSE method and (b) TTIm calibration method

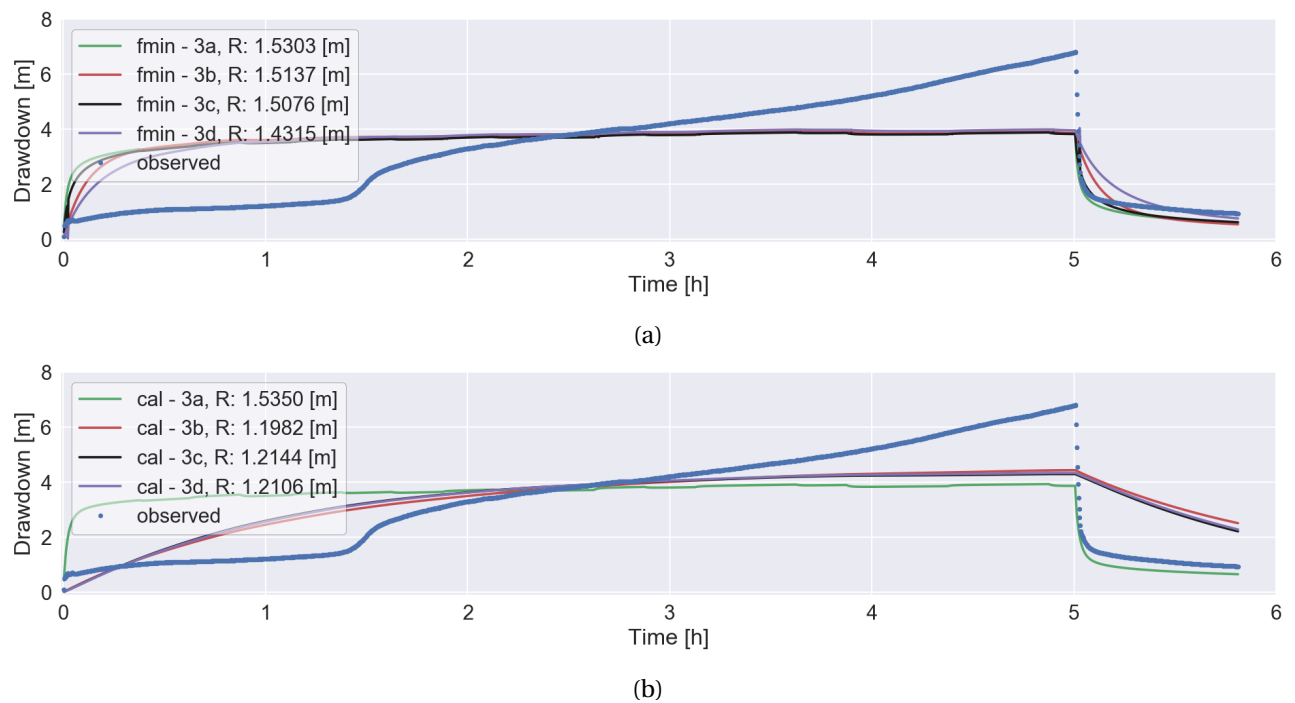
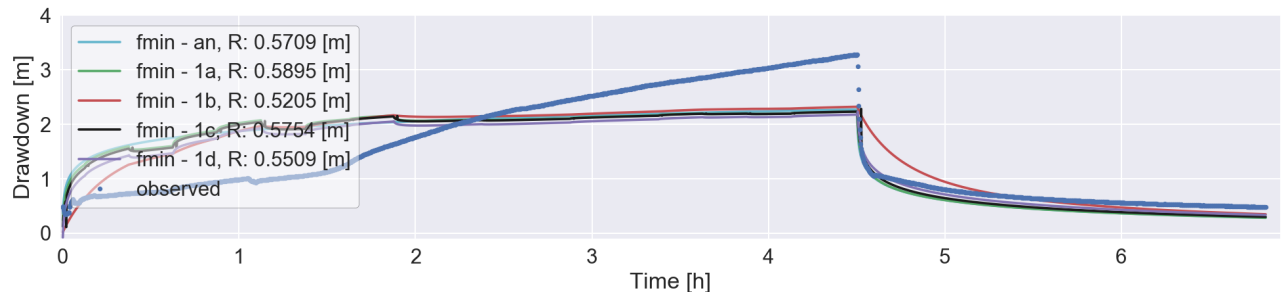


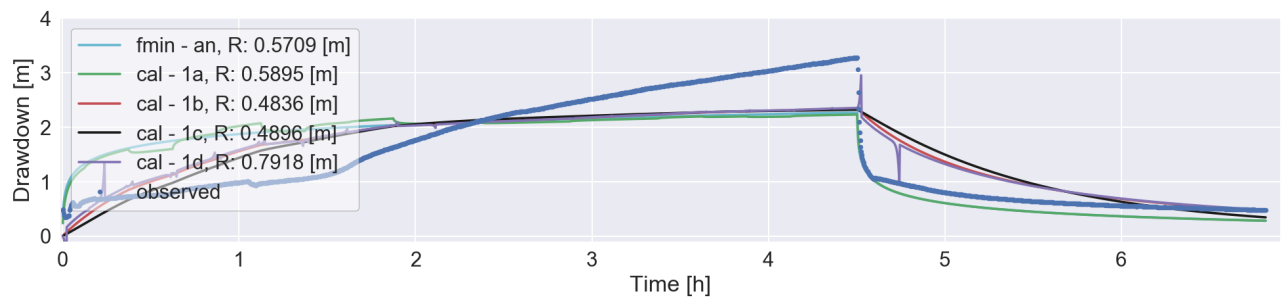
Figure C.9: Janga first attempt partially penetrating double layer fieldwork data analysis (a) fmin-RMSE method and (b) TTIm calibration method

594

C.5. Janga second attempt - overview

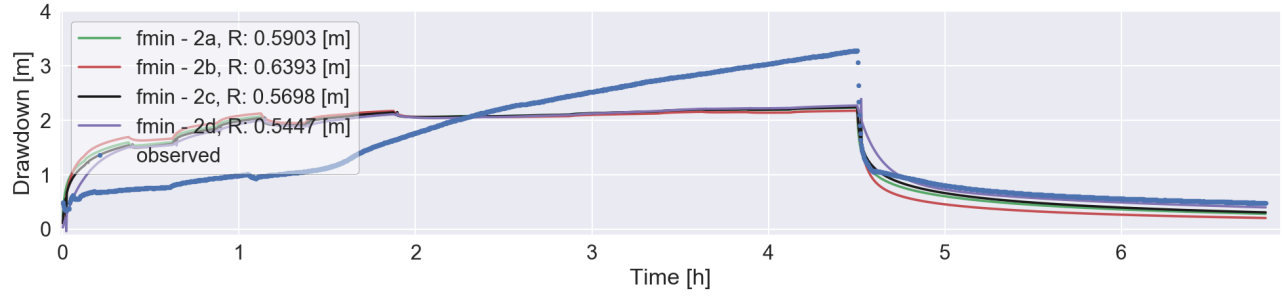


(a)

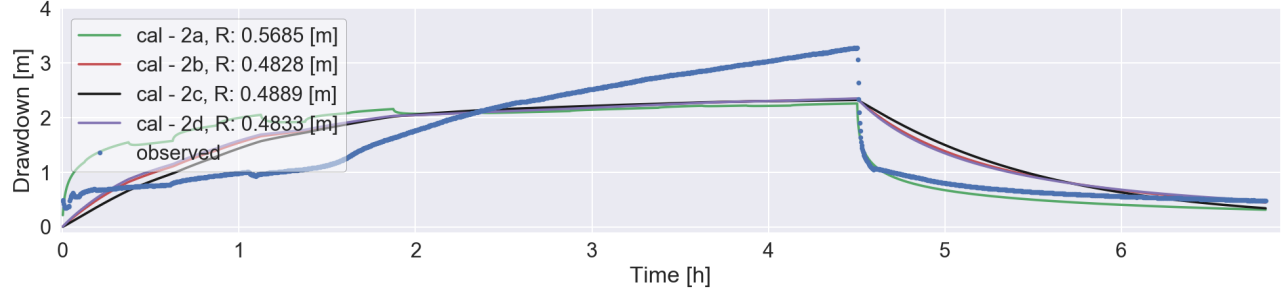


(b)

Figure C.10: Janga second attempt single layer fieldwork data analysis by the optimization (a) fmin-RMSE method and (b) TTIm calibration method



(a)



(b)

Figure C.11: Janga second attempt double layer fieldwork data analysis by the optimization (a) fmin-RMSE method and (b) TTIm calibration method

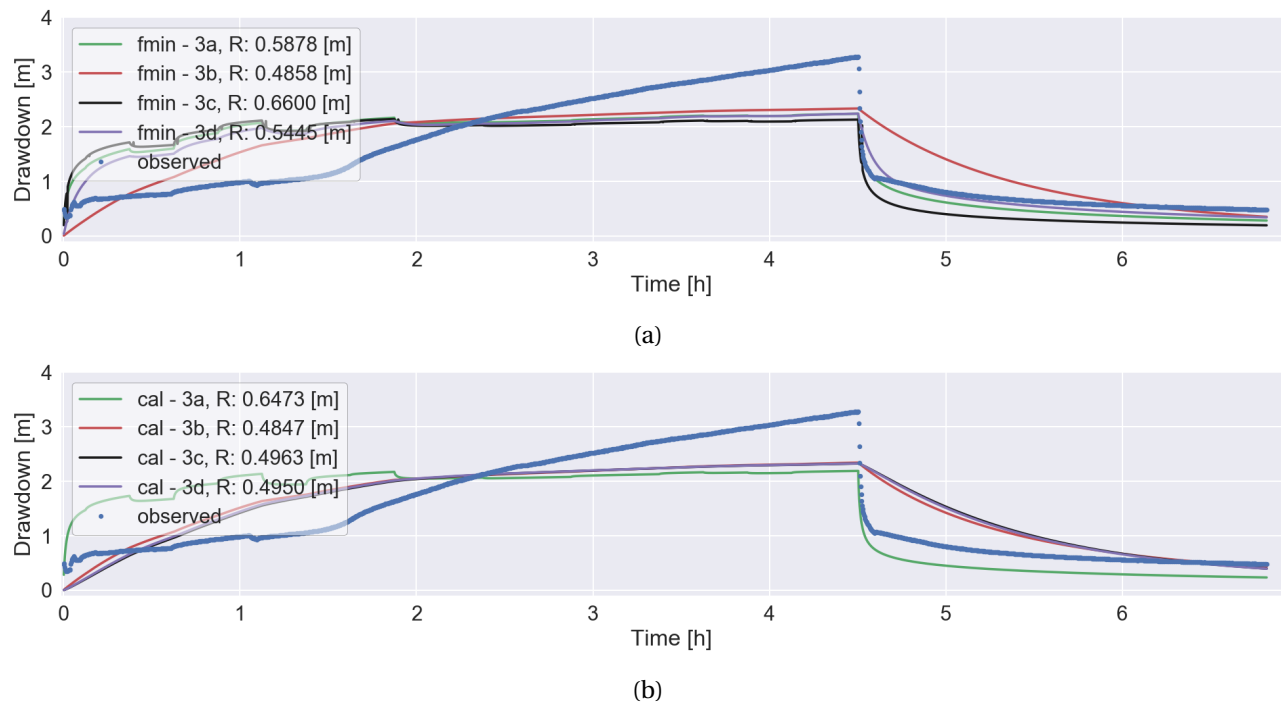
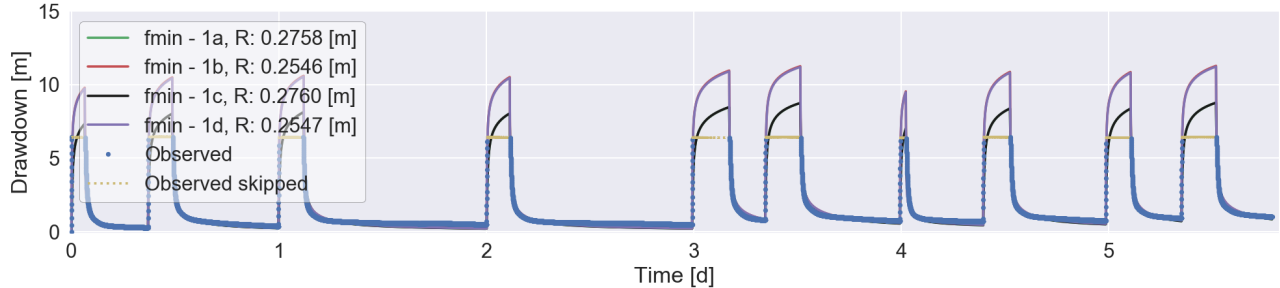
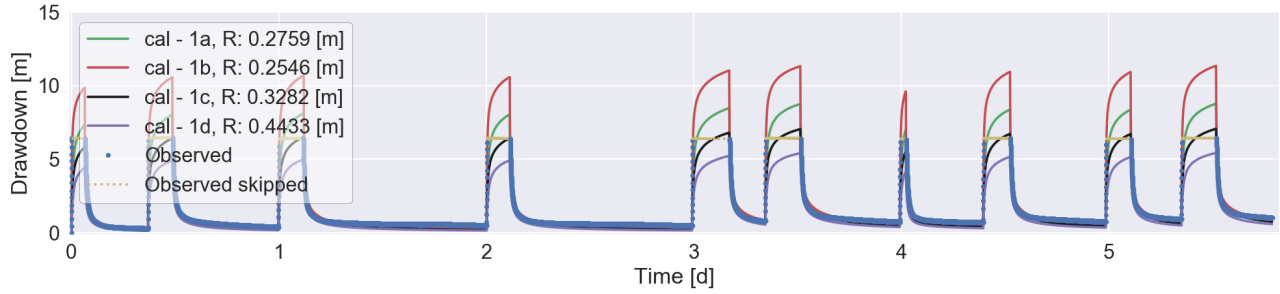


Figure C.12: Janga second attempt partially penetrating double layer fieldwork data analysis by the optimization (a) fmin-RMSE method and (b) TTIm calibration method

595 **C.6. Ziong - overview**

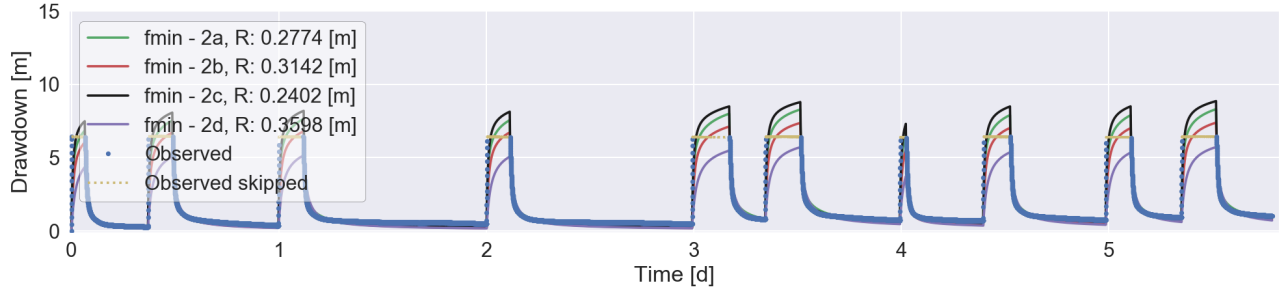


(a)

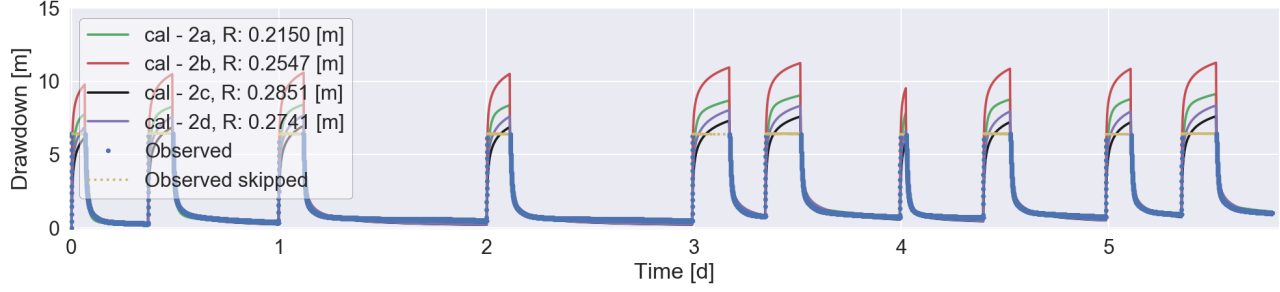


(b)

Figure C.13: Ziong single layer fieldwork data analysis by the optimization (a) fmin-RMSE method and (b) TTIm calibration method



(a)



(b)

Figure C.14: Ziong double layer fieldwork data analysis by the optimization (a) fmin-RMSE method and (b) TTIm calibration method

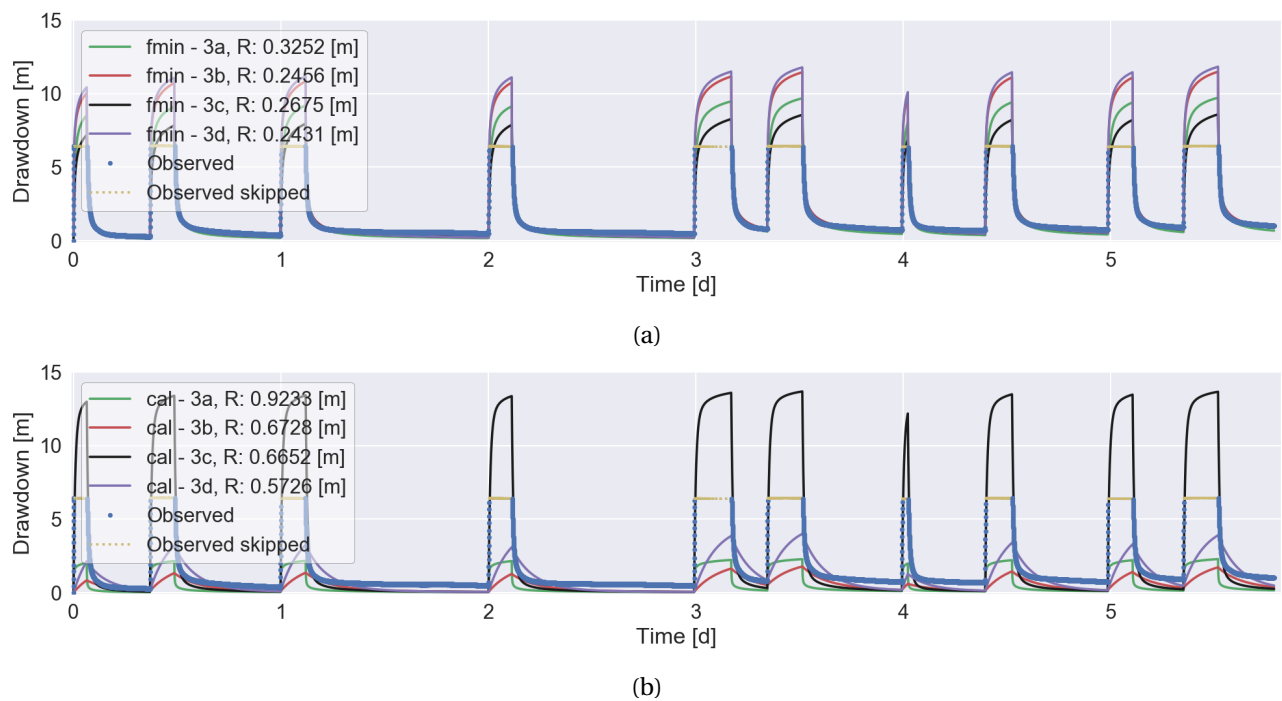


Figure C.15: Ziong partially penetrating double layer fieldwork data analysis by the optimization (a) fmin-RMSE method and (b) TTim calibration method

D

596

597

Modflow radial conversion

598 Introduction

599 The general thesis topic is pointed at the groundwater flow around a well. Due to seasonal circumstances
600 the same well acts both as extraction and injection well. Direction of groundwater flow is alternately pointed
601 towards and away from the well. This phenomenon can be simulated straightforward by the use of the
602 USGS's modular hydrologic model MODFLOW. To generate adequate results in groundwater fluctuations
603 high model accuracies are desirable, especially close to the well. The model preferably accommodates a
604 fine-meshed grid by the implementation of a multitude of rows and columns. As a consequence model
605 runtimes will last long.

606 However, groundwater flow around a well can (under specific conditions) be approached as a phenomenon
607 of radial symmetry. Minor radial parameter conversions can reduce the number of dimensions in the MOD-
608 FLOW model. A modification that reduces model runtimes substantially (Langevin, 2008). The section be-
609 low contains a detailed description of the required radial scaling of parameters, as applied in this thesis. In
610 addition, three examples are included to test and compare the radial scaled model performance.

611 Theoretical method

612 MODFLOW is naturally based on rectangular geometry. Without the inclusion of specific adjustments this
613 results in (multi layered) rectangular models. Model shapes not by definition necessary in the case of a
614 well simulation. Under the assumption of subsurface conditions to be homogeneous and the absence of
615 elements disturbing the regional hydraulic gradient it is possible to interpret the groundwater flow around
616 a well as a phenomenon strictly cylindrical. Assumptions on which one would approach well flow model
simulation as being axially symmetric (Figure D.1).

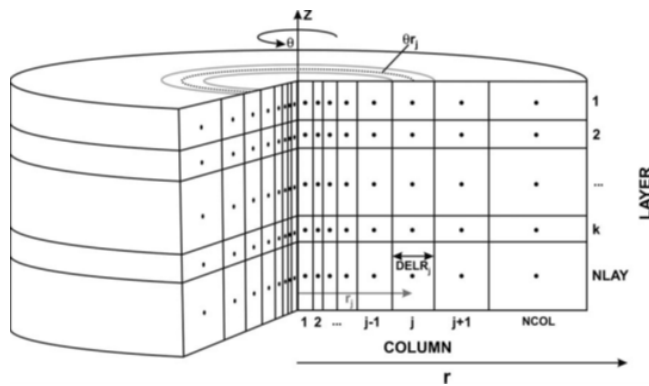


Figure D.1: Schematic of an axially symmetric model (Langevin, 2008)

617

618 The in figure D.1 displayed cylindrical approach of a well model can be simulated by an MODFLOW model
619 (rectangular geometry) which accommodates one or more layer(s), one row only and multiple columns. In
620 this single row model it is assumed the well is included in the first column. Moreover, the single row should

act as the representation of a subsurface slice. This is achieved by the radial modification of multiple parameters. Radial parameter scaling guarantees the conversion of a rectangular (single row) MODFLOW model into a fictive radial model. Elaborating on the explanation of Langevin (2008) the following parameters become radial dependent:

$$K_h \rightarrow K_{h,j}^* = K_{h,j} \theta r_j \quad (\text{D.1})$$

$$K_v \rightarrow K_{v,j}^* = K_{v,j} \theta r_j \quad (\text{D.2})$$

$$S_s \rightarrow Ss_j^* = Ss_j \theta r_j \quad (\text{D.3})$$

$$S_y \rightarrow Sy_j^* = Sy_j \theta r_j \quad (\text{D.4})$$

$$n \rightarrow n_j^* = n_j \theta r_j \quad (\text{D.5})$$

Where K_h and K_v represent the horizontal and vertical hydraulic conductivity, S_s is the specific storage, S_y is the specific yield (phreatic storage) and n is the porosity. Scaled parameters modification is highlighted by the introduction of the superscript *. As visible by the subscript j the parameters hereby become column (radial) dependent. r_j is the radial distance between column j and the well (column 1) and θ is the angle of the representing slice. For the purpose of radial scaling θ covers a complete ring; $\theta == 2\pi$.

Main advantage of the implementation of the radial parameter conversion is the reduction in model dimensions. At local scale (close to well) the model can contain a detailed meshed-grid without the emergence of excessive model runtimes. Moreover the parameter is applied within the common modelling program MODFLOW itself, no specialized programs are required. However, it has to be mentioned the circular model approach can only be applied under the specific assumptions of radial symmetry (Langevin, 2008).

Test application

To validate the radial scaled model performance, a total of three fictive test exercises are applied. In these exercises a comparison is made between the radial scaled model (Figure D.2c) and two natural rectangular based MODFLOW models (Figure D.2a and Figure D.2b). The rectangular MODFLOW model is the most straightforward. Due to the squared shape deviations in model outcome are expected. Whereas the rectangular round MODFLOW model is manually circularized. This model accommodates the gradual increase in flow area in the radial direction. Based on Langevin (2008) it is expected the rectangular round model should approximate radial model outcomes.

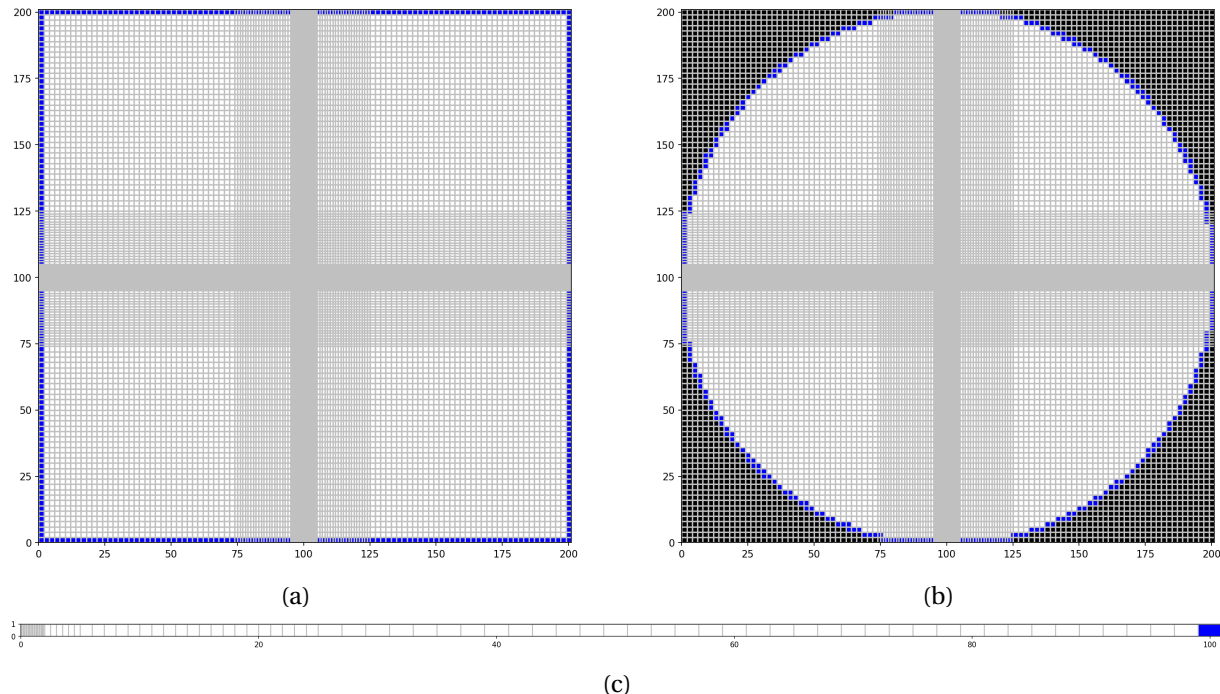


Figure D.2: MODFLOW topview schematisation of a: (a) Rectangular model, (b) Rectangular round model and (c) Single row model
 (grey = cell boundary, red = well position, blue = boundary condition, black = inactive cell)

644 The exercises applied deliberately show strong similarities with the first two test problem cases described
 645 by Langevin (2008). In terms of content the exercises are designed with the same set of parameters, making
 646 it possible to validate the results in general. As an exception a small deviation is applied in terms of grid def-
 647 inition. In these exercises the cell sizes increase (grouped) stepwise based on an increasing (radial) distance
 648 from the well. By the use of the cell sizes 0.1 (20x), 0.5 (6x), 1.0 (20x) and 2.0 m (38x) a total model length
 649 (radial length) of 101 m is simulated. This grid structure is applicable on the single row (radial) model. The
 650 rectangular and rectangular round model accommodate a same and corresponding grid structure, as visible
 651 in the model top views of figure D.2.

D.1. Test 1: Steady flow to a fully penetrating well in confined aquifer

The steady state solution of a confined aquifer fully penetrated by a well is applied as a first MODFLOW model performance test. The exercise schematic configuration is depicted in the overview of figure D.3. The case is characterized by its simplicity, making it an exercise ideally suitable for the comparison against the analytical solution. Thiem's method (Equation D.6) is applied as the analytical drawdown solution for radial well flow in a confined aquifer (Krusseman & de Ridder, 2000):

$$S_j = \frac{Q \ln(\frac{r_2}{r_j})}{2\pi K_{(h)} H} \quad (\text{D.6})$$

Where S_j is the drawdown in column j , Q is the discharge, $r_2 = 100$ m (constant head at a distance of in this case 100 m from the well), r_j is the radial distance between column j and the well (column 1), $K_{(h)}$ is the horizontal hydraulic conductivity and H is the aquifer thickness.

Decline in groundwater head due to well behaviour can also be expressed directly by the use of the analytical discharge potential (strack, 1989), as depicted in (Equation D.7). Applied on confined conditions it is assumed $H = h_0$ (Source?? geo1). As a result confined heads can be determined by the application of equation D.9. Outcomes in head are in complete correspondence with the drawdown calculated by Thiem's method.

$$\phi_j = \frac{Q}{2\pi} \ln\left(\frac{r_j}{R}\right) + \phi_0 \quad (\text{D.7})$$

$$h_j = \frac{\phi_j}{k_h H} \quad (\text{D.8})$$

$$h_j = \frac{\phi_j}{k_h H} \quad (\text{D.9})$$

Where ϕ_j is the discharge potential at column j , Q is the discharge, $R = 100$ m (constant head (h_0) at a distance of in this case 100 m from the well), r_j is the radial distance between column j and the well (column 1), $K_{(h)}$ is the horizontal hydraulic conductivity and H is the aquifer thickness.

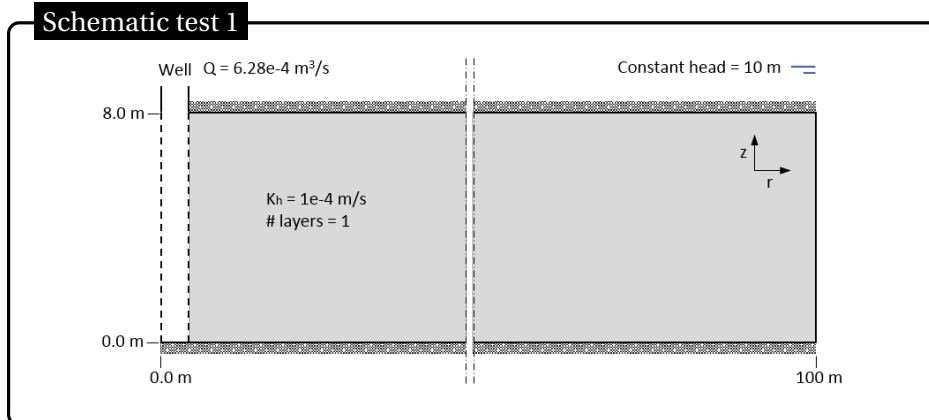


Figure D.3: Schematic test 1

The rectangular MODFLOW model overestimates drawdown (modelled heads are slightly lower) compared to the analytical solution. This difference can be explained by the rectangular shape of the model; imposed boundary condition along the model edge (especially the corners) are positioned 'outside' the defined radial boundary of 100 m from the well. The rectangular round model works around this inconvenience, and already shows more similarities with the analytical solution. Some deviation in the first meter(s) around the well still exist, which can potentially be attributed to the cell structure. These minor deviations are no longer present by the application of the radial scaled (single row) model. Regardless the (radial) position, modelled heads and drawdown are identical to the analytical solution. A first indication the radial scaled MODFLOW model is preferential applicable on this thesis purposes.

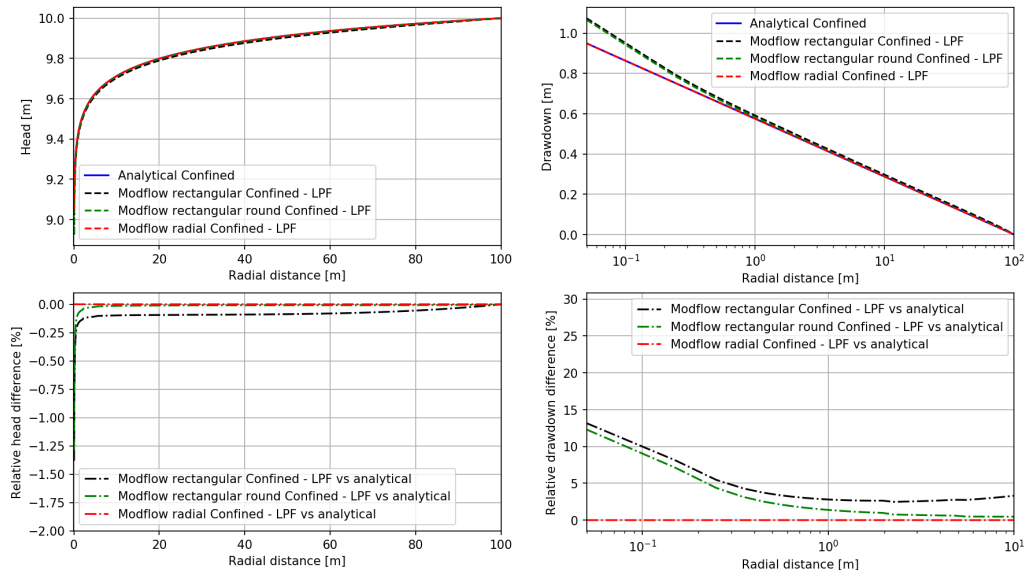


Figure D.4: Results test 1

D.2. Test 2: Steady flow to a fully penetrating well in unconfined aquifer

Example exercise two (Figure D.5) accommodates the same test problem as depicted in test 1, only exception is the transition towards unconfined aquifer conditions. In this example the analytical drawdown solution presented by the Thiem-Dupuit's method for steady-state flow to a fully penetrating well in an unconfined aquifer is used as a reference(Kruseman & de Ridder, 2000):

$$S'_j = \frac{Q \ln(\frac{r_2}{r_j})}{2\pi K_{(h)} D} \quad (\text{D.10})$$

$$S'_j = S_j - \frac{S_j}{2D} \quad (\text{D.11})$$

Where S'_j is the uncorrected drawdown in column j, S_j is the iteratively corrected drawdown in column j, Q is the discharge, $r_2 = 100$ m (constant head at a distance of 100 m from the well), r_j is the radial distance between column j and the well (column 0), $K_{(h)}$ is the horizontal hydraulic conductivity and D is the thickness between aquifer bottom and constant head. For the purposes of this exercise the analytical drawdowns are iteratively determined with a precision of 1e-6.

Also under unconfined conditions the analytical discharge potential (Equation D.12) can be applied (Strack, 1989). Only exception, compared to the confined conditions, is the minor change in head derivation, visualised in D.14. Major advantage, with respect to the analytical Thiem-Dupuit's method, is the absence of the iterative head derivation process. Result is the analytical calculation of even more accurate heads by the application of the discharge potential.

$$\phi_j = \frac{Q}{2\pi} \ln\left(\frac{r_j}{R}\right) + \phi_0 \quad (\text{D.12})$$

$$\phi_0 = \frac{1}{2} k_h h_0^2 \quad (\text{D.13})$$

$$h_j = \sqrt{\frac{2\phi_j}{k_h}} \quad (\text{D.14})$$

Where ϕ_j is the discharge potential at column j, Q is the discharge, $R = 100$ m (constant head (h_0) at a distance of in this case 100 m from the well), r_j is the radial distance between column j and the well (column 1), $K_{(h)}$ is the horizontal hydraulic conductivity and H is the aquifer thickness.

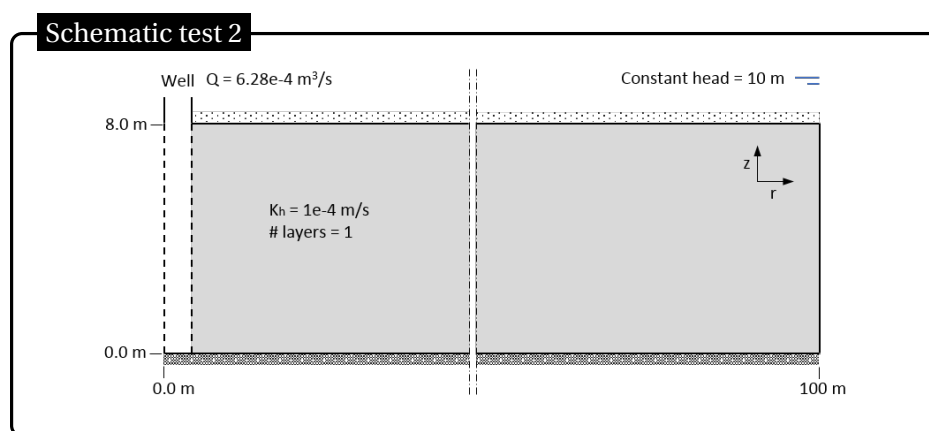


Figure D.5: Schematic test 2

Due to a 10 m constant head boundary the aquifer area of flow is fictive enlarged in the unconfined case (compared to the 8 m aquifer height under confined conditions). In accordance with the solutions in Langevin (2008) overall drawdowns in the unconfined conditions are slightly lower with respect to the confined situation. Model performances of the unconfined example exercise show similar behaviour as the

704 confined example exercise. Differences in modelled and analytical determined heads and drawdowns are
 705 minuscule in general. As expected largest deviations from the analytical solution are present in the MOD-
 706 FLOW rectangular model. The differences in outcome of this model do persist over almost the entire radial
 707 distance from the well, regardless the use of the BCF or LPF package. Although it is only slightly, the use
 708 of the LPF package shows slightly better performance. For the purposes of this thesis the LPF package is
 709 assumed to be preferential in setting the aquifer properties. Application of this package in the MODFLOW
 710 round rectangular model results in improved model results, however deviations do continue to exist. In
 711 contrast with the confined exercise (D.1) application of the radial scaled MODFLOW model under uncon-
 712 fined aquifer conditions deviations from the analytical solution are still present. Modelled drawdowns show
 713 strong similarities with the uncorrected analytical solution. Moreover, relative to the analytical solution the
 714 absolute radial scaled MODFLOW model outcomes performs most accurately. Making the radial scaled
 715 (single row) MODFLOW model suitable for the unconfined aquifer conditions of this thesis.

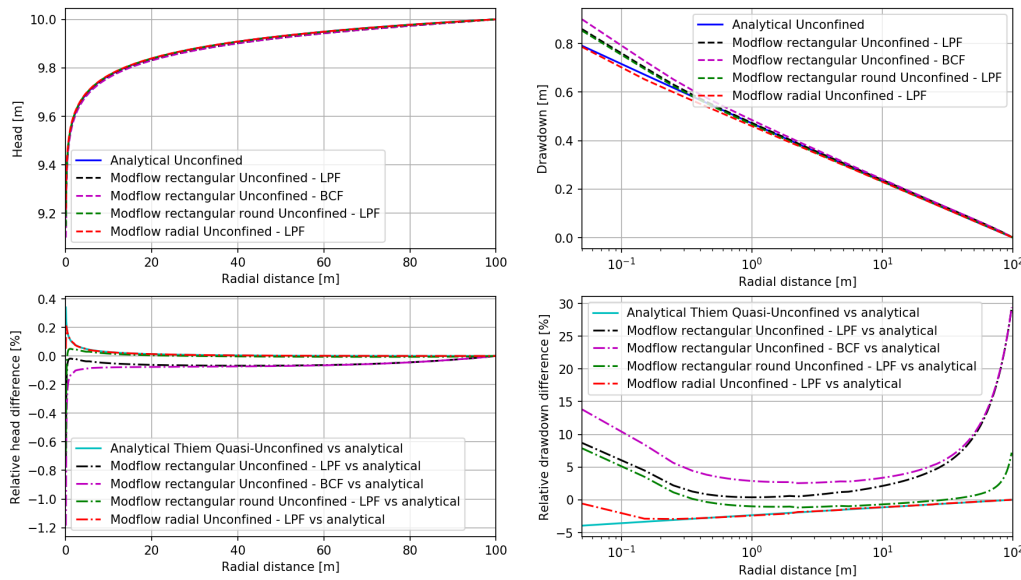


Figure D.6: Results test 2

716 D.3. Test 3: Unsteady flow to a partially penetrating well in unconfined aquifer

717 As a final exercise the different MODFLOW models are subjected to a more complicated case (Figure D.7).
 718 This specific exercise includes all model parameters dependent on radial scaling to test the overall radial
 719 model performance. This case accommodates a well which is partially penetrating the aquifer, making it a
 720 multi-layered problem. Sum up of the fractional discharges of the penetrating layers (48-72) results in the
 721 total well discharge. Moreover the exercise is time dependent. In this case all results are obtained after one
 722 day of groundwater withdrawal.

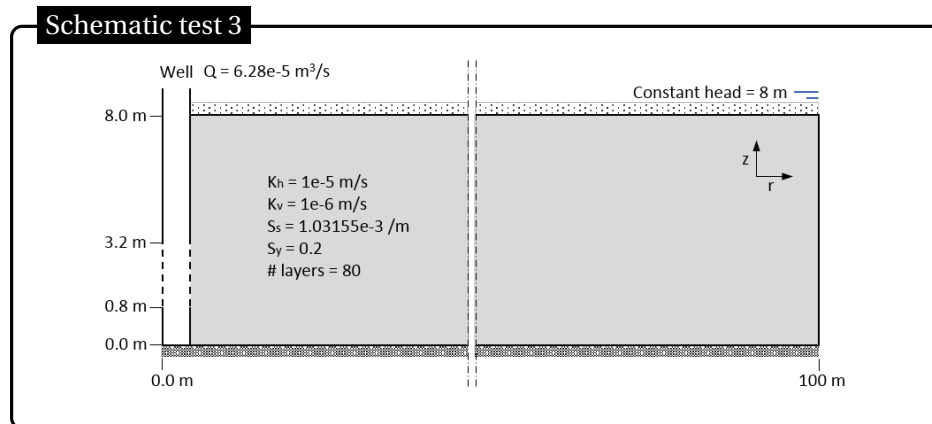


Figure D.7: Schematic test 3

723 Performance of the radial scaled (single row) MODFLOW model is visualized by the head contour plot in fig-
 724 ure D.8. From the perspective of proper comparison results of the different models are in this case shown
 725 at an height of 2.0 m (relative to aquifer bottom) along the entire aquifer (Figure D.9). Outcome of the com-
 726 parative study is a scaled (single row) radial model which performs as expected. With the exception of the
 727 first meter(s) around the well differences between the rectangular round and the radial MODFLOW models
 728 are negligible small. Deviations at close range to the well can be attributed to the chosen grid structure.
 729 Based on the test exercises 1 and 2 it can be assumed the results of the radial model simulates the natural
 730 well behaviour properly. Application of the radial scaled (single row) MODFLOW model with the use of the
 731 LPF package is a relative fast and suitable model for this thesis purposes.

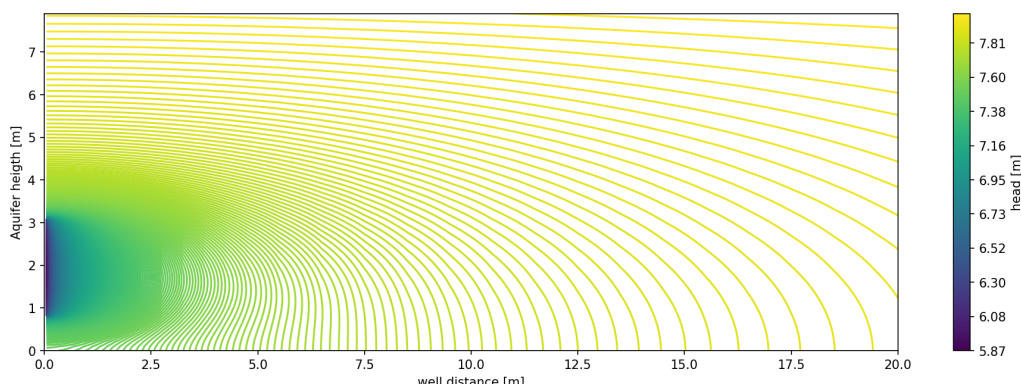


Figure D.8: Results test 3: Cross-section head contour after 1 day of pumping

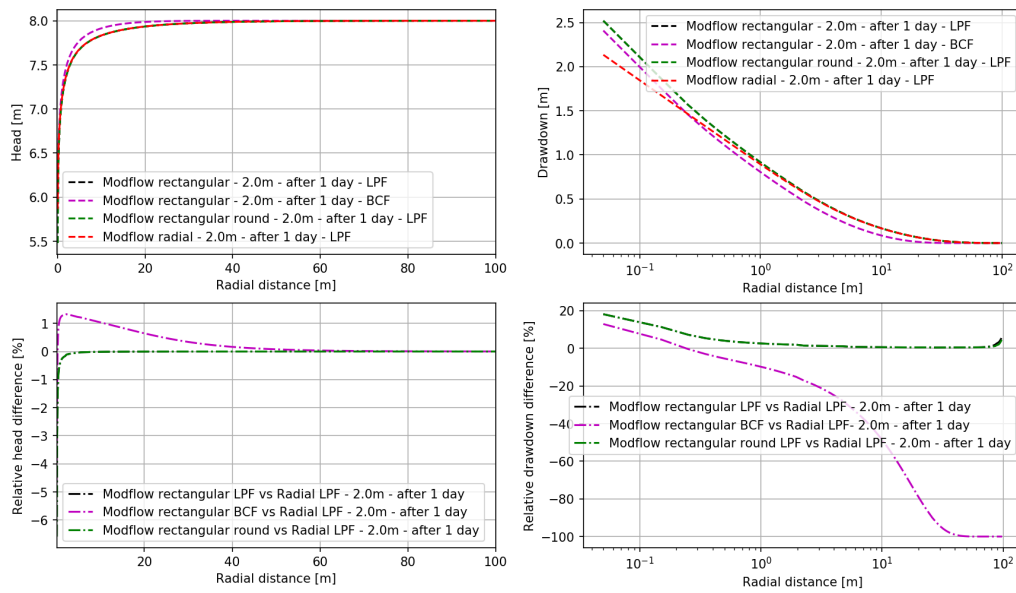


Figure D.9: Results test 3: Head after 1 day of pumping at 2.0m (relative to aquifer bottom)